Global and Planetary Change 66 (2009) 129–148

Contents lists available at ScienceDirect

Global and Planetary Change

journal homepage: www.elsevier.com/locate/gloplacha

Coral reef evolution on rapidly subsiding margins

Jody M. Webster [a,b,*], Juan Carlos Braga [d], David A. Clague [c], Christina Gallup [e], James R. Hein [f], Donald C. Potts [g], Willem Renema [h], Robert Riding [i,1], Kristin Riker-Coleman [e], Eli Silver [j], Laura M. Wallace [k]

[a] School of Geosciences, The University of Sydney, Sydney, NSW 2006, Australia
[b] School of Earth and Environmental Sciences, James Cook University, Townsville, Qld 4811, Australia
[c] Monterey Bay Aquarium Research Institute, Moss Landing, California, USA
[d] Departamento de Estratigrafia y Paleontologia, Universidad de Granada, Spain
[e] Department of Geological Sciences, University of Minnesota Duluth, Duluth, Minnesota, USA
[f] U.S. Geological Survey, Menlo Park, CA, USA
[g] Department of Ecology and Evolutionary Biology, University of California, Santa Cruz, California, USA
[h] Nationaal Natuurhistorisch Museum, Leiden, The Netherlands
[i] School of Earth, Ocean and Planetary Sciences, Cardiff University, Cardiff CF10 3YE, UK
[j] Department of Earth and Planetary Sciences, University of California, Santa Cruz, CA, USA
[k] GNS Science, Lower Hutt, New Zealand

ARTICLE INFO

Article history:
Received 1 April 2008
Accepted 31 July 2008
Available online 30 November 2008

Keywords:
carbonate platforms
coral reefs
drowning
sedimentary facies
Pleistocene sea-level change
meltwater pulse events
Hawaii
Papua New Guinea

ABSTRACT

A series of well-developed submerged coral reefs are preserved in the Huon Gulf (Papua New Guinea) and around Hawaii. Despite different tectonics settings, both regions have experienced rapid subsidence (2–6 m/ka) over the last 500 ka. Rapid subsidence, combined with eustatic sea-level changes, is responsible for repeated drowning and backstepping of coral reefs over this period. Because we can place quantitative constraints on these systems (i.e., reef drowning age, eustatic sea-level changes, subsidence rates, accretion rates, basement substrates, and paleobathymetry), these areas represent unique natural laboratories for exploring the roles of tectonics, reef accretion, and eustatic sea-level changes in controlling the evolution of individual reefs, as well as backstepping of the entire system. A review of new and existing bathymetric, radiometric, sedimentary facies and numerical modeling data indicate that these reefs have had long, complex growth histories and that they are highly sensitive, recording drowning not only during major deglaciations, but also during high-frequency, small-amplitude interstadial and deglacial meltwater pulse events. Analysis of five generalized sedimentary facies shows that reef drowning is characterized by a distinct biological and sedimentary sequence. Observational and numerical modeling data indicate that on precessional (20 ka) and sub-orbital timescales, the rate and amplitude of eustatic sea-level changes are critical in controlling initiation, growth, drowning or sub-aerial exposure, subsequent re-initiation, and final drowning. However, over longer timescales (>100–500 ka) continued tectonic subsidence and basement substrate morphology influence broad scale reef morphology and backstepping geometries. Drilling of these reefs will yield greatly expanded stratigraphic sections compared with similar reefs on slowly subsiding, stable and uplifting margins, and thus they represent a unique archive of sea-level and climate changes, as well as a record of the response of coral reefs to these changes over the last six glacial cycles.

1. Introduction

Recent investigations of drowned Quaternary coral reefs in rapidly subsiding margin settings such as the “Big Island” Hawaii and the Huon Gulf of Papua New Guinea, indicate that these systems contain a unique, and largely unexploited, archive of reef drowning and backstepping, sea-level variations, and climate changes (Webster et al., 2004a; Webster et al., 2007). Despite representing different tectonics settings, a foreland basin (Huon Gulf) and a hotspot (Hawaii) (Fig. 1), these regions have experienced rapid subsidence (2–6 m/ka) over the last 500 ka, and thus constitute a unique natural laboratory for exploring the relationship between tectonics, reef accretion, and eustatic sea-level changes in controlling the reef evolution.

Unlike their transgressive and highstand fossil counterparts, that developed in stable (e.g., Great Barrier Reef, Florida Margin, Bahama Bank) and uplifted settings (e.g., the Huon Peninsula, Barbados, Ryukyu Islands, and Red Sea), the submerged reefs of the Huon Gulf and Hawaii are mainly glacial reefs that developed in response to rapid

* Corresponding author. School of Geosciences, The University of Sydney, NSW, 2006, Australia. Tel.: +612 9036 6538; fax: +612 9351 0184.
E-mail address: jody.webster@usyd.edu.au (J.M. Webster).
[1] Present address: Department of Earth and Planetary Sciences, University of Tennessee, Knoxville, Tennessee, USA.

0921-8181/$ – see front matter © 2008 Elsevier B.V. All rights reserved.
doi:10.1016/j.gloplacha.2008.07.010

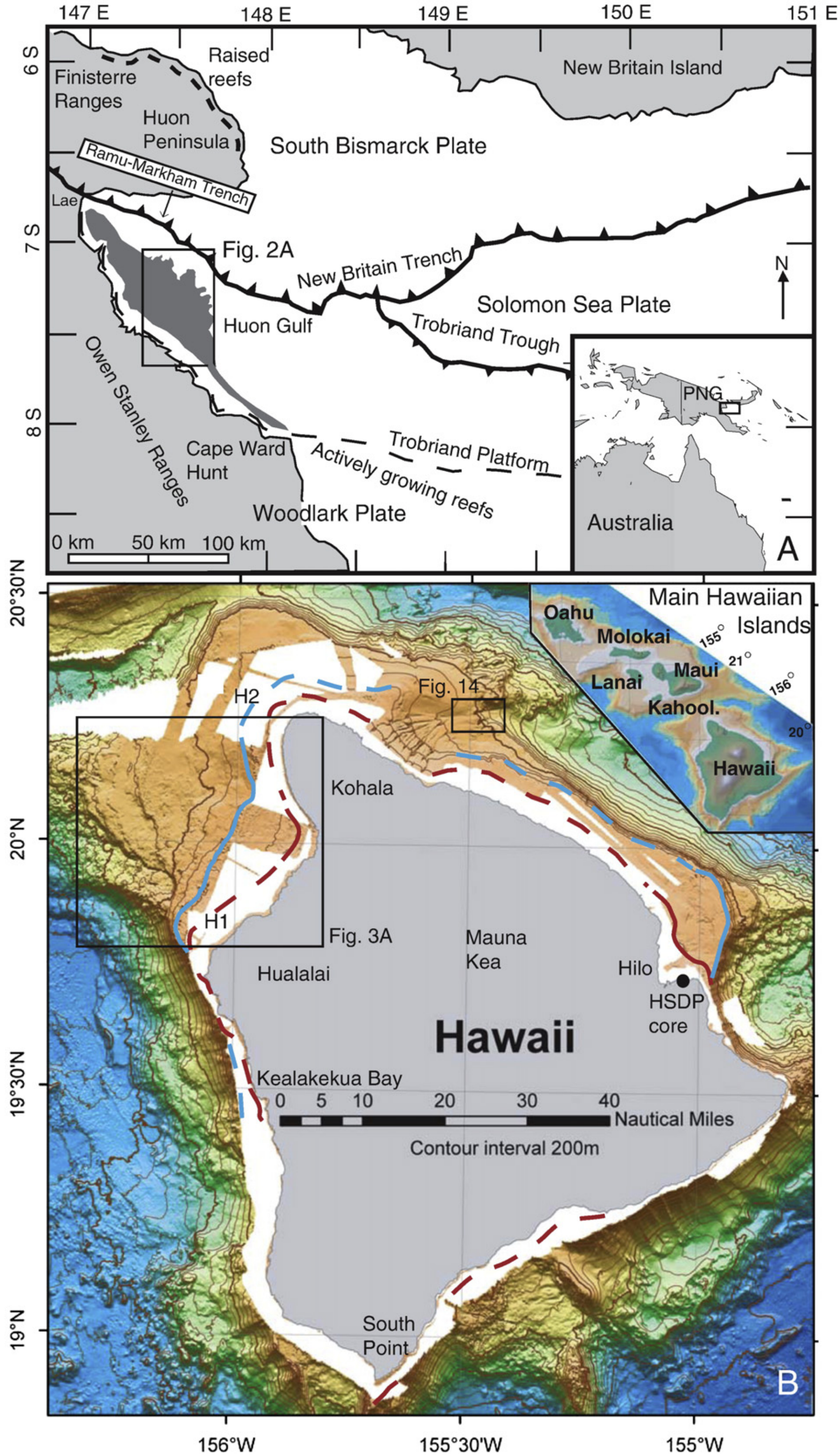

Fig. 1. Regional location map showing the study areas. (A) Huon Gulf (PNG) showing the drowned coral reefs (grey shaded area); modern fringing reef (dashed line); Trobriand platform (long dashed line); and uplifted raised reef terraces (thick dashed line) along the Huon Peninsula. Rectangle outlines the study area detailed in Fig. 2 (after Webster et al., 2004c). (B) The "Big Island" of Hawaii showing the drowned coral reefs. The known (solid line) and probable (dashed line) extent of the −150 m (H1, in red) and (H2, in blue) −400 m drowned reefs are also shown. Rectangles outline the main study areas detailed in Figs. 3 and 14 (after Clague et al., 1998; MBARI Mapping Team, 2000; Webster et al., 2004a). (For interpretation of the references to colour in this figure legend, the reader is referred to the web version of this article.)

subsidence (~2–6 m/ka) (Moore and Fornari, 1984; Ludwig et al., 1991; Galewsky et al., 1996; Wallace, 2002). Depending on the relationship between eustatic sea-level changes and reef growth, rapid subsidence ensures accommodation space is continually created, thus generating greatly expanded stratigraphic sections compared to reefs from stable and uplifting tectonic settings. Recent drilling investigations around the island of Tahiti (Montaggioni et al., 1997; Cabioch et al., 1999; Camoin et al., 2007) have also revealed expanded stratigraphic reef sections that grew in response to subsidence – albeit at a much lower rate (0.15 to 0.4 m/ka) (Montaggioni, 1988; Pirazzoli and Montaggioni, 1988) than Hawaii and the Huon Gulf.

Drowned reefs in rapidly subsiding settings also develop during other periods of Earth's sea-level and climate history (i.e., glacial periods, early deglaciations) that are inadequately sampled by reefs in stable and uplifting tectonic settings. Previous workers on Hawaii (Moore and Fornari, 1984) and Papua New Guinea (Galewsky et al., 1996) speculated that reef initiation occurred during periods of stable sea-level in the highstands and continued throughout the regressions before finally drowning during the early part of the deglaciations. The tops of the coral reefs are, therefore, particularly sensitive to eustatic sea-level rise and should encapsulate a clear sedimentary signature of reef drowning that can be observed, characterized, and compared with extant bio-sedimentary facies and, more crucially, interpreted within a precise ^{14}C and U/Th chronologic framework. Unlike most other ancient carbonate platforms and reefs it is possible to place realistic quantitative constraints (i.e., of eustatic sea-level changes, subsidence rates, drowning times, carbonate accretion rates, and paleobathymetry) on these depositional systems allowing direct links to be established between fundamental processes and their morphological, stratigraphical and sedimentary response.

We review and synthesize new and existing bathymetry, dive observations, sedimentary facies, radiometric and numerical modeling data from two of the best-studied drowned reef systems on rapidly subsiding margins – the Huon Gulf and Hawaii. We discuss the implications of these data for understanding the main factors controlling their: (1) structure and morphology, (2) sedimentary facies composition and transitions, (3) drowning and backstepping, and (4) internal stratigraphical successions. Finally, we discuss the potential of these reefs, particularly in Hawaii, as a new IODP drilling target.

2. Regional setting and rapid subsidence

2.1. Huon Gulf, Papua New Guinea

The Australian plate converges obliquely with the Pacific plate, producing a complex and active system of micro-plates and associated vertical and lateral movements. In the Huon Gulf, the South Bismarck plate collides with and overrides the northern Australian continental margin (Davies et al., 1987a,b; Pigram and Davies, 1987; Abbott et al., 1994a,b) (Fig. 1A). A classic fore-deep has developed on the lower plate of the convergence zone in the Huon Gulf (Galewsky et al., 1996) with a complex series of 14 reefs, pinnacles, and banks now preserved 100 to 2500 m below sea-level (Webster et al., 2004b). U/Th dating of corals (details in Section 5) from the drowned reef at −2000 m (348 ka) and −250 m (60 k) constrain the rate of subsidence between 2 and 6 m/ka (Galewsky et al., 1996; Webster et al., 2004b) (Fig. 2).

Based on observational and numerical modeling data, Galewsky (1998) and Wallace (2002) argued that subsidence within the Huon Gulf is driven by plate flexure caused by the foreland-migration of the subduction load at a rate of ~60 mm/yr (Wallace et al., 2004). As a result of plate flexure, the rate of subsidence varied through time and space as the subsidence rates are highest closest to the subduction load. Superimposed on this general northeast downward flexing towards the trench, Webster et al. (2004b) found that the deep (>−1000 m) reefs have also been systematically tilted ~15 m/km towards the northwest, and the shallow reefs (<−300 m) tilted ~2 m/km towards the southwest. They concluded that post-depositional reef tilting is related to the location of the centroid of the encroaching thrust mass (the Finisterre Range) to the NW (Fig. 2A), and to possible spatial variations in the flexural rigidity of the underlying lithosphere.

Along the adjacent Huon Peninsula, on the overriding South Bismarck plate, the Finisterre collision has caused uplift (1–3 m/ka) and preservation of a complementary sequence of raised coral reef terraces (Chappell, 1974) (Fig. 1A). The Finisterre collision was initiated between 3.7 and 3.0 Ma (Abbott et al., 1994b), and rates of uplift since this time have been high. The Oligocene and Early Miocene volcanic rocks of the Finisterre Range are overlain by Neogene and Quaternary marine carbonates that have been folded into a broad anticline. Dating and paleobathymetric studies of the carbonate rocks show that tectonically-driven surface uplift rates of these carbonates were approximately 1–2 m/ka (Abbott et al., 1997), similar to rates measured for the raised Huon Peninsula reef terraces. The co-existence of the uplifted Huon Peninsula reefs and the subsided Huon Gulf reefs at the same plate boundary provides a rare, complementary record of reef evolution on uplifting and subsiding margins.

2.2. Hawaii – the big island

The Hawaiian Archipelago, in the central Pacific Ocean, formed from a relatively stationary hotspot that built volcanic islands on the northwest moving Pacific plate (Wilson, 1963). The subsidence of Hawaii is caused by lithospheric loading associated with continued volcanism over this hotspot during the last 500 ka (Moore, 1987). Previous investigations of the drowned reefs off northwest Hawaii (Moore and Fornari, 1984; Moore and Campbell, 1987; Ludwig et al., 1991; Webster et al., 2004a) indicate a mean, long-term subsidence rate of 2.5–2.6 m/ka over that period. Based on the depth below sea-level and age of the subaerial-submarine basalt transition (at 1079 m and 402 ± 50 ka) observed in core HSDP-2 (Fig. 1B), Sharp and Renne (2006) calculated a similar subsidence rate of 2.7 ± 0.7 m/ka for the eastern side of Hawaii (Hilo). Caccamise et al. (2005) observed that the short-term rates (measured by GPS over six years) are significantly less than the longer-term rates (estimated geologically), but this difference may be related to processes that could vary on short timescales.

In contrast to the foreland basin setting of the Huon Gulf, the long term subsidence rates experienced by the reefs in Hawaii have probably been uniform over the last 250 ka, at least in the primary NW study area (Figs. 1B and 3A). For example, the subsidence rate in Hawaii is a direct result of the size of the load (the volcanoes) and the rheology of the lithosphere. Since neither the load nor the rheology change rapidly, the rate of sinking is fairly constant over thousands of years (Moore, 1987; Moore and Clague, 1992). The location of the center of the load shifts to the southeast slowly over time as new volcanoes are added to the southeast end of the chain and the older volcanoes to the northwest cease their activity. This complexity means that most of the reefs across Hawaii are tipped down towards the southeast after they have drowned. This situation is minimized in the main study area (Figs. 1B and 3A) because the orientations of the drowned reefs are close to perpendicular to the trend of the chain.

3. Reef structure and morphology

High-resolution bathymetric and sidescan data, combined with ROV and submersible observations, show significant differences in the gross structure and morphology of reefs between the Huon Gulf and Hawaii that include reef number, shape and sinuosity. However, both locations record clear evidence of similar primary growth features, localized mass wasting and composite or multigenerational reef structures.

3.1. Reef number and morphology

Webster et al. (2004b) mapped and characterized 14 distinct reefs and numerous pinnacles and banks in the Huon Gulf. The reefs vary in sinuosity, but all trend NW–SE, parallel to the Ramu–Markham Trench and the present Morobe coastline (Fig. 2A), and preserve morphological features indicating primary reef growth (e.g., raised reef crests, lagoons, spur and grooves, patch reefs and mounds) (Fig. 2B–E). The reef margins form a complex system of promontories and re-entrants

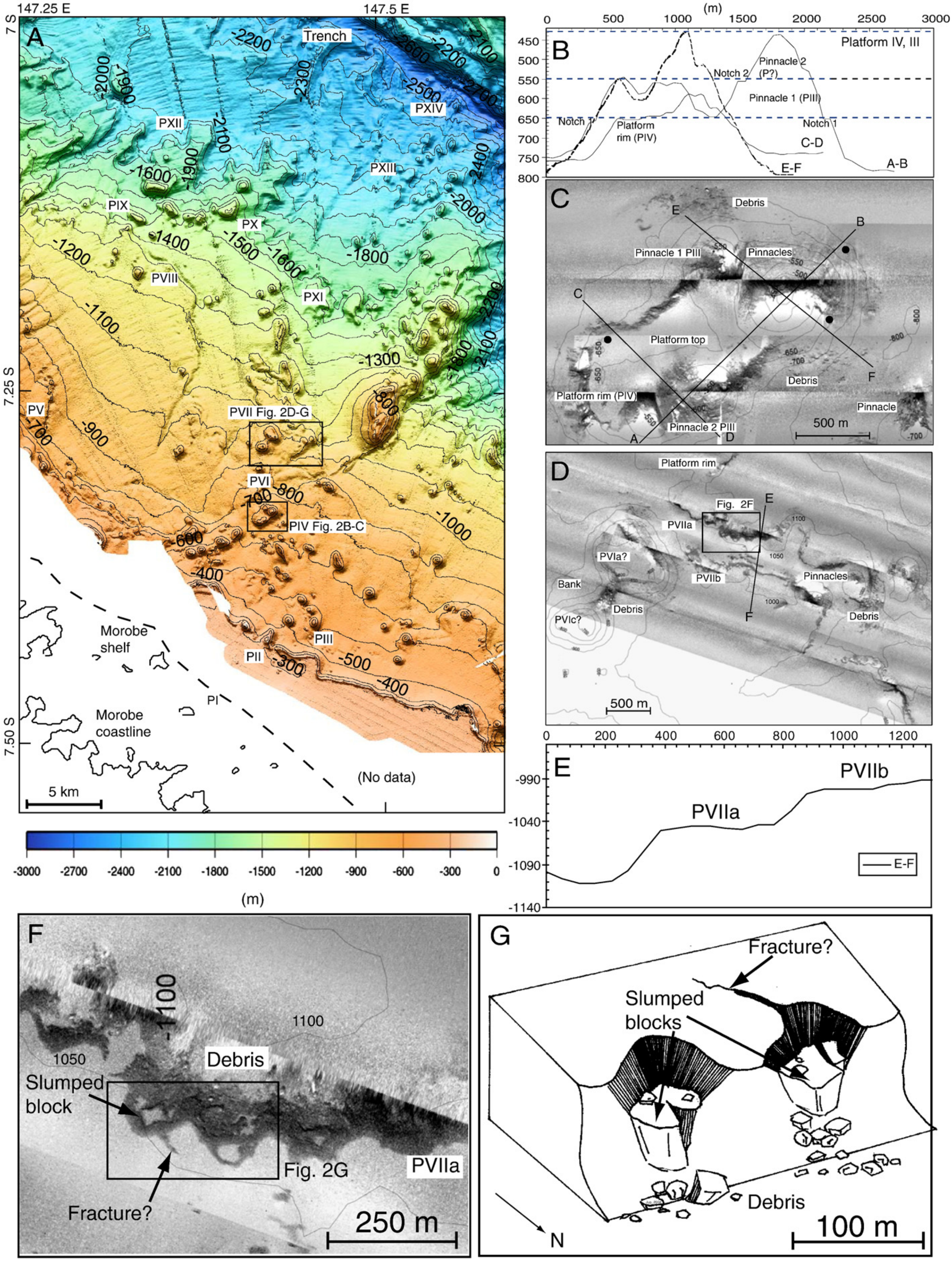
A
B
C
D
E
F
G
147.25 E
147.5 E
7 S
7.25 S
7.50 S
Trench
PXII
PXIV
PXIII
PIX
PX
PXI
PVIII
PV
PVII Fig. 2D-G
PVI
PIV Fig. 2B-C
PIII
PII
PI
Morobe shelf
Morobe coastline
(No data)
5 km
(m)
Platform IV, III
Pinnacle 2 (P?)
Notch 2
Pinnacle 1 (PIII)
Notch 1
Platform rim (PIV)
C-D
E-F
A-B
Debris
Pinnacle 1 PIII
Pinnacles
Platform top
Platform rim (PIV)
Pinnacle 2 PIII
Pinnacle
500 m
Platform rim
Fig. 2F
PVIIa
PVIa?
PVIIb
Bank
PVIc?
250 m
Slumped block
Fracture?
Fig. 2G
Fracture?
Slumped blocks
100 m
N

(up to 5 km), with abundant pinnacles and banks at similar depths lying seaward of the main reefs (Fig. 2D). This configuration closely mimics the complex morphology of the present Huon Gulf coastline, seaward islands and shoals, and demonstrates the roles of original geology and basement topography in influencing reef development (Fig. 2A).

Twelve reefs have been mapped around Hawaii and eleven of those off the northwest coast (Figs. 1B and 3A) (after Moore and Fornari, 1984; Ludwig et al., 1991; Clague et al., 1998; MBARI Mapping Team, 2000; Webster et al., 2004a). Compared with the Huon Gulf these reefs are significantly less sinuous, with H2 and H1 appearing to wrap smoothly around part of the Kohala peninsula. Currently incomplete shallow bathymetric data makes it difficult to confidently trace any of the reefs around the island. However, the available bathymetry and DEM data east of Kohala volcano (Figs. 1 and 3A) shows the reefs becoming more compressed or narrower, perhaps in response to steeper basement substrates as implied by the steep slope of the onshore topography (Fig. 3A). Similar to the Huon Gulf, outcrop-scale ROV/sub observations and bathymetry data reveal structures resembling original spurs and grooves, elevated reef rims and flats, as well as patch reefs or mounds within landward lagoons (Fig. 3B,C).

3.2. Evidence of mass wasting

Sidescan data and ROV observations show that localized mass wasting is common along the margins of the Huon Gulf reefs. Larger debris fields up to 0.6×0.3 km are observed along the flanks of steep reef margins and high-relief banks and pinnacles (Fig. 2B,F). The debris consists of fragments of reef limestone, derived from the upper reef and pinnacle margins. Linear fractures or joints up to 2 m apart trend both parallel and perpendicular to the reef rim. The intersections of these fracture sets "dissects" the reef margin forming angular blocks up to ~80 m wide that are transported down slope. Fig. 2D,F and G illustrates this mass wasting process. The Hawaiian reefs show similar evidence of localized mass wasting, with eroded scarps and substantial debris and talus at the base of some forereef slopes.

Without direct age control, we cannot determine whether mass wasting occurred coevally with deposition of the reefs, or after they drowned. Apart from a few local exceptions (pinnacle flanks and canyon heads in the Huon Gulf), the data suggest that mass wasting has generally removed <100 m of material laterally from the seaward margin of the main reefs since their deposition (Webster et al., 2004b). Moore and Clague (1987) estimated a similar amount of mass wasting and landward retreat of the shallowest and youngest reef (H1) offshore in Hawaii. However, larger volumes of material may be buried beneath hemipelagic sediments at the base of the reef slopes. Additional high resolution seismic and radiometric data are required to quantify the debris volume, better constrain the rates and timing of erosional processes and identify possible causes of reef margin collapse (e.g., seismic shocks, sediment loading and oversteepening, and tsunamis).

3.3. Composite or multigenerational reef structures

The bathymetry data reveal that the Huon Gulf and Hawaiian reefs are composite features, consisting of multiple terrace levels and associated benches (Figs. 2B,D,E and 3C,D), separated vertically by 10 to 50 m. At least three processes could explain the formation of these terraces and benches. First, they could be erosional features, formed at lower sea-levels and preserved following sea-level rise. Given the high subsidence rates (2–6 m/ka), this is unlikely, as relative sea-levels were not stable long enough to erode extensive terraces. Second, they could have formed by localized post-depositional normal faulting. However, the seismic data from the Huon Gulf do not support this hypothesis (Galewsky et al., 1996; Webster et al., 2004b). Third, they could be depositional features formed during multiple phases of reef growth and drowning, and small-scale backstepping during as many sea-level oscillations.

The multigenerational reef structures are spatially continuous across considerable distances on some reefs (e.g., Huon Gulf reefs PXII, PVI and PIV; Hawaiian reefs H1, H8), but across other reefs (e.g., PVII) the continuity is less clear. Seismic data from the Huon Gulf support the idea that reef histories are complex, with multiple phases of growth preserved. The data also confirm that these features can be buried by sedimentary cover, explaining why, in some places, they are difficult to correlate spatially from bathymetric and sidescan data alone. Additional bathymetric, seismic, and radiometric data are necessary before we can confirm the origin of these composite features. However, we suggest that they represent multiple phases of construction and drowning during high-frequency, low-amplitude interstadial/stadial sea-level cycles (details below).

4. Sedimentary facies and signatures of reef drowning

4.1. Sedimentary facies and paleoenvironmental settings

Analysis of over 700 samples recovered from the Huon Gulf and Hawaiian reefs has revealed a diverse suite of sedimentary facies (after Galewsky et al., 1996; Webster et al., 2003; Webster et al., 2004a; Webster et al., 2004c; Webster, 2006; Webster et al., 2007). In this review, we recognize five generalized sedimentary facies that are common to both systems. The main components of these facies, their stratigraphic relationships and paleoenvironmental significance are summarized below.

4.1.1. Facies 1: Shallow coral reef (0–20 m)

The shallow coral reef facies is dominated by in-situ coralgal frameworks (i.e., bindstones, framestones, bafflestones) and represents the main reef-building facies within both systems. In the Huon Gulf, two distinct coral assemblages constitute this facies: (1) a shallow (0–5 m), high energy reef community of robust branching *Acropora* sp. (i.e., *A. palifera*, *A. humilis* group, Fig. 4A,B) characteristic of windward margins and, (2) another shallow community composed of encrusting *Montipora* sp. that indicates less exposed, lower energy reef conditions. A quantitative re-analysis (Tager et al., in press) of the taxonomic composition of the coral communities that form this facies found that they were significantly different from their uplifted, highstand counterparts previously reported from the nearby Huon Peninsula (Pandolfi, 1996). In Hawaii, the shallow coralgal frameworks are characterized by massive *Porites lobata* (Fig. 4C), and robust branching *P. compressa* (Fig. 4D), with associated encrusting *Montipora* and *Leptastrea* colonies.

Nongeniculate coralline algal crusts are an abundant part of the framework of this facies at both sites. They are dominated by mastophoroid algae such as *Neogoniolithon fosliei* (Fig. 4E,F) and *Hydrolithon onkodes* (Fig. 4F) that commonly occur as 2–40 mm layers sandwiched between encrusting corals and overgrowing massive and

Fig. 2. Main study in the Huon Gulf (PNG). (A) High resolution multibeam bathymetry data showing the drowned reefs (P1-PXIV). Rectangles outline locations of two representative high-resolution (DSL-120) sidescan sonar surveys. (B) Bathymetric profiles crossing raised reef rim and lagoon of PIV (625–670 m). (C) Sidescan image of the PIV reef rim, flat-topped bank, steep pinnacles, associated benches and limestone debris on the pinnacle flanks. The location of bathymetric profiles in (B) are also shown. (D) Sidescan image of PVII showing two distinct reefs (PVIIa, 1050 m and PVIIb, 1000 m) ~400 m apart, with numerous shallower landward pinnacles and banks. (E) Bathymetric profile (from Fig. 2D) showing multigenerational reef structure of PVII. (F) Enlarged side scan image of PVIIa showing evidence of mass wasting (i.e., fractures, slumped blocks, and debris) along the reef margin. (G) Interpretive sketch of Fig. 2F, rotated 180° and viewed from the northeast to show mass wasting (after Webster et al., 2004b).

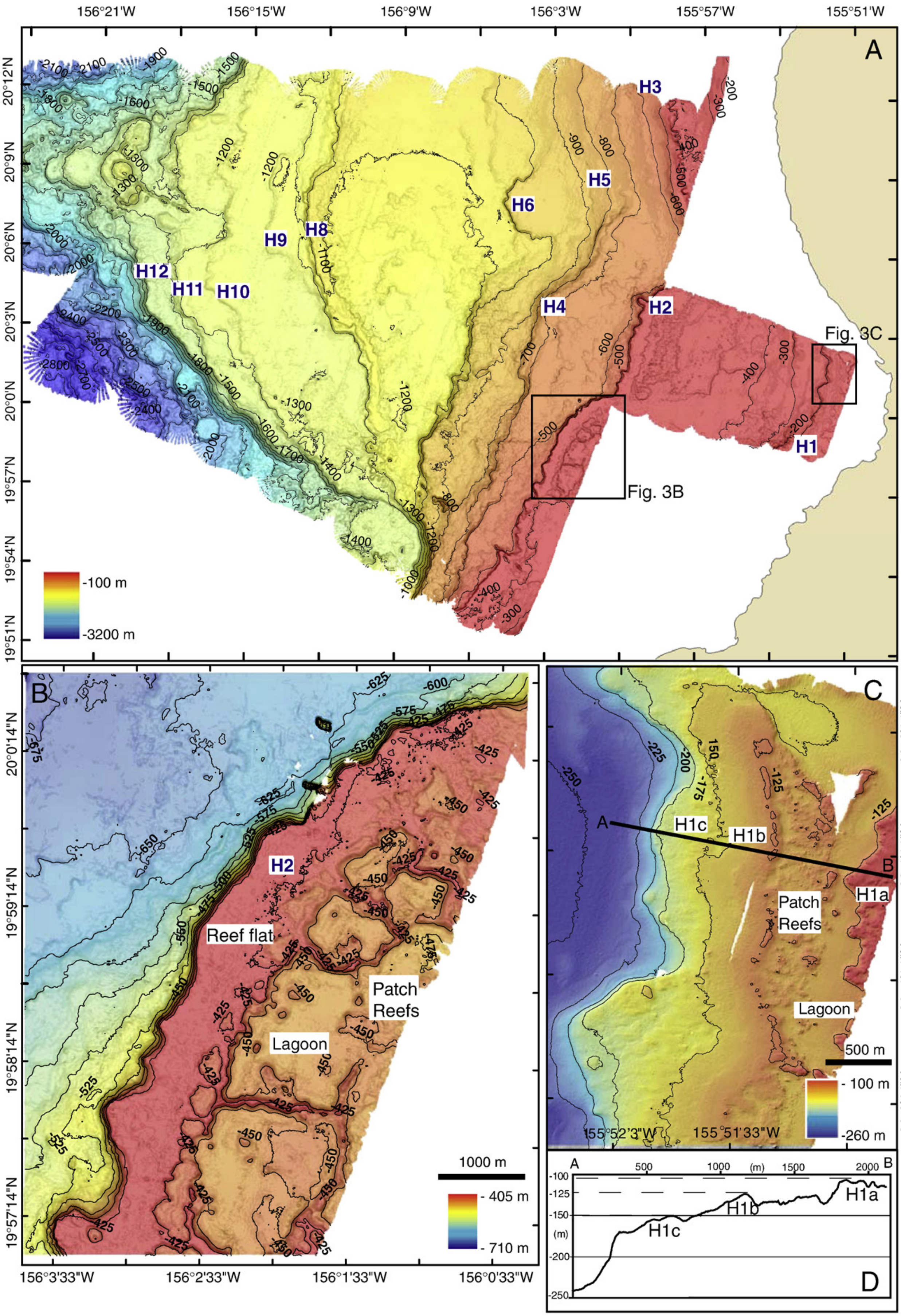
A
B
C
D
156°21'W
156°15'W
156°9'W
156°3'W
155°57'W
155°51'W
20°12'N
20°9'N
20°6'N
20°3'N
20°0'N
19°57'N
19°54'N
19°51'N
H1
H2
H3
H4
H5
H6
H8
H9
H10
H11
H12
Fig. 3B
Fig. 3C
-100 m
-3200 m
H2
Reef flat
Patch Reefs
Lagoon
1000 m
- 405 m
- 710 m
156°3'33"W
156°2'33"W
156°1'33"W
156°0'33"W
20°0'14"N
19°59'14"N
19°58'14"N
19°57'14"N
H1a
H1b
H1c
Patch Reefs
Lagoon
500 m
- 100 m
-260 m
155°52'3"W
155°51'33"W
20°2'14"N
20°1'44"N
20°1'14"N
20°0'44"N
(m)
500
1000
1500
2000

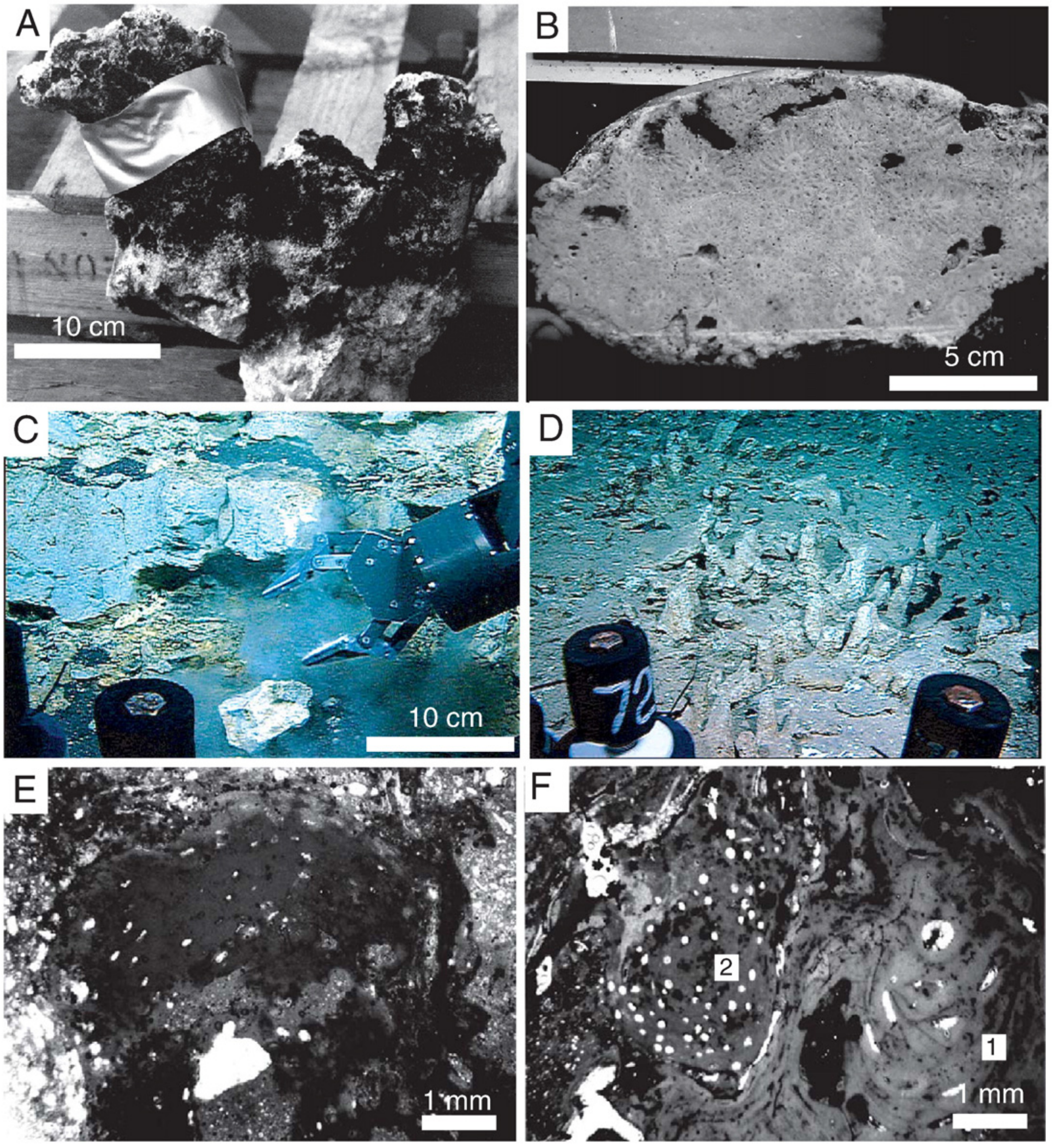

Fig. 4. Sedimentary facies deposited in shallow coral reef settings (Facies 1: 0–20 m). (A–B) Shallow, high energy coral assemblage from the Huon Gulf reefs with robust branches of *Acropora palifera* (A) (PX11, −1980 m, PNG) and *Acropora* cf. *humilis*? (B) (PXIII, −2124 m, PNG). (C) Outcrop photo showing an in-situ massive *Porites lobata* exposed at the base of Hawaiian reef H7 in the Kohala plunge pool (H7, −967 m, Hawaii, see also Fig. 14). (D) Outcrop photo showing in-situ robust branching *Porites compressa* with truncated flat tops on the reef crest of Hawaiian reef H8a (−1197 m, Hawaii). (E) Photomicrograph showing well-developed crusts of nongeniculate mastophoroid coralline algae *Neogoniolithon* sp. (PIV, −733 m, PNG). (F) Photomicrograph showing well-developed crusts of nongeniculate mastophoroid coralline algae *Neogoniolithon fosliei* (1) and *Hydrolithon onkodes* (2) (PVIIb, 1113 m, PNG) (after Webster et al., 2004c; Webster, 2006).

branching corals. Large shallow-water benthic foraminifera *Amphisorus* and *Peneroplis* are also common within this facies. Comparisons with modern Indo-Pacific reefs suggest this facies is characteristic of shallow coral reef settings, usually <10–15 m of water, and certainly <20 m.

4.1.2. Facies 2: Intermediate coralgal crust/nodule (20–60 m)

The intermediate coralgal facies is characterized by floatstones and bindstones comprised of coralline algae and minor corals that commonly overlie the shallow-water coral reef facies. This facies forms irregular nodules (2–5 cm diameter) or crusts on hard substrates composed of thick fruticose (warty) layers of coralline algae (e.g., *Lithothamnion prolifer*, *Mesophyllum erubescens*, *Lithophyllum acrocamptum,* and *Hydrolithon munitum*) growing either around nuclei of shallow-water origin (e.g., bored corals) (Fig. 5A) or associated with thin in-situ encrusting/foliaceous corals (*Leptoseris, Pavona, Montipora*) (Fig. 5B). Other components include coralline algal branches, large *Halimeda* segments, bryozoans, large benthic foraminifera (*Heterostegina depressa, Amphistegina. radiata, A. lessonii*, and *Operculina*) and bivalve fragments (Fig. 5C,D). Taken together this assemblage of corals, coralline algae and benthic foraminifera is characteristic of intermediate fore-reef slope environments in −20 to −60 m of water.

Fig. 3. Main study area off the northwest coast of Hawaii. (A) High resolution multibeam bathymetry data showing the drowned reefs (H1–H12). Rectangles outline areas detailed in Fig. 2B, C. (B) Close up showing the morphologic details of H2. (C) Close up showing the morphologic details of H1. (D) Bathymetric profile (A–B) across H1 showing three distinct reefs (H1a at −105 m; H1b at −125 m; H1c at −150 m) (after Clague et al., 1998; MBARI Mapping Team, 2000; Webster et al., 2004a).

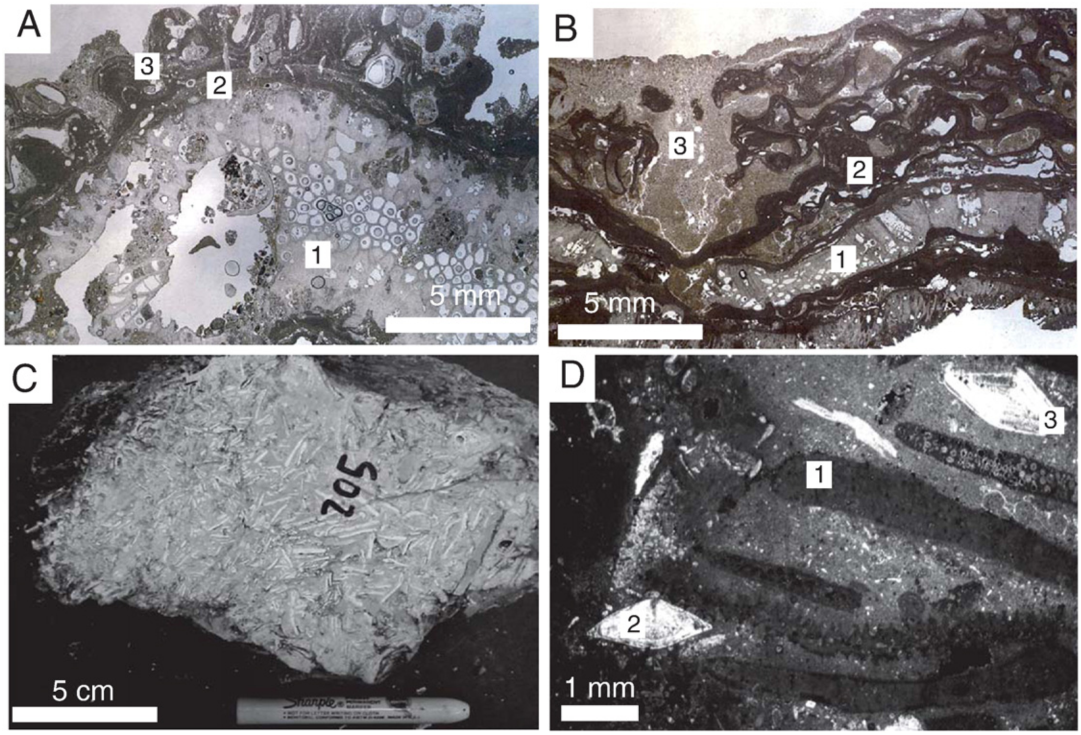

Fig. 5. Sedimentary facies deposited in intermediate fore-reef slope settings (Facies 2: −20 to −60 m). (A) Photomicrograph of a coralline algal nodule with a coral (Pocilloporiid) nucleus (1), and a deepening algal sequence from an inner crust dominated by *Hydrolithon munitum* and acervulinid foraminifera (shallow assemblage) (2) to an outer crust of *Lithophyllum pustulatum* and fruticose *Mesophyllum* (3) (intermediate assemblage) (H7, −997 m, Hawaii). (B) Photomicrograph of a coralgal bindstone with thin encrusting Agariciid corals (*Pavona* sp. (1) and *Leptoseris* sp.), encrusted by *Lithophyllum pustulatum* gp, fruticose *Mesophyllum erubescens* (2), *Lithoporella* and *L. pustulatum* which is bored and infilled with hemipelagic sediments (H7, −936 m, Hawaii). (C) *Halimeda* floatstone with numerous segments or plates “floating” within a micrite matrix (PXI, −1650 m, PNG). (D) Photomicrograph of a *Halimeda* (1) floatstone with abundant large benthic foraminifera, *Amphistegina lessonii* (2) and A. *radiata* (3) (PVIII, −1281 m, PNG) (after Webster et al., 2004c; Webster, 2006).

4.1.3. Facies 3: Coralline algal-foraminiferal crust/nodule (60–120 m)

The coralline algal-foraminiferal crust/nodule facies is characterized by coralline algal and foraminiferal crust-dominated bindstones, nodular floatstones and rudstones. This facies is common in Hawaii on horizontal surfaces (e.g., the original reef crest) where it forms a distinct crust or pavement (Fig. 6A,B). In the Huon Gulf, it can form substantial low-lying, meter-scale, hummocky structures. At both locations, the facies consists of either sub-spherical nodules or crusts on hard substrates (Fig. 6C,D), composed of complex, multi-generational crusts that form an open framework of melobesioid coralline algae (*Lithothamnion*, *Mesophyllum)* (Fig. 6E) with *Sporolithon, Lithoporella,* and *Peyssonnelia* sp., interspersed with micrite, and abundant encrusting acervulinid foraminifera (Fig. 6F,G). In the Huon Gulf, this facies is also characterized by the occurrence of the large benthic foraminiferan *Cycloclypeus carpenteri* that is commonly found at depths of −60 to −120 m in modern settings (Iryu et al., 1995; Hohenegger et al., 2000). At thin section, hand specimen, and outcrop-scales, this facies overlies the intermediate fore-reef slope facies. Comparison with modern algal-foraminiferal frameworks in the Indo Pacific (see Davies et al., 2004 for a review) suggests deposition in a deep fore-reef slope setting between −60 m to −120 m.

4.1.4. Facies 4: Microbial (>120–150 m?)

Below 120 m, all reef-building corals and most coralline algae have ceased active growth. In Hawaii, living coralline algae may live below this depth, but only as millimetre-scale crusts lacking reproductive structures (Braga et al., 2005). In these deep open-platform settings, the drowned Huon Gulf and Hawaiian reefs are characterized by a complex succession of: (1) a microbial carbonate facies followed by, (2) a hemipelagic/pelagic facies and finally (3) a zone of intense boring, infilling and Fe–Mn precipitation (Fig. 7). Similar successions have been reported from reef rocks dredged from −80 m and −130 m off Tahiti and the Marquesas Islands, and interpreted as reflecting deepening and changing water quality associated with a rapid deglacial sea-level rise (Camoin et al., 2006).

We identify two main microbial fabrics forming the microbial facies in the Huon Gulf and Hawaiian drowned reefs. The first forms peloidal sediment infilling cavities (Fig. 7A,C) and the second forms laminated peloidal and clotted micrite crusts up to 5 cm thick, in some places, forming complex, digitate stromatolitic overgrowths (Fig. 7E). A recent review by Camoin et al. (2006) found that microbial carbonate sediments can occur in shallow and deep-water reef settings, but in the Huon Gulf and Hawaiian reefs there is clear stratigraphic evidence that the microbialites postdate the deep-water (60–120 m) coralline-algal facies (e.g., Fig. 7A,E) and must have been deposited at greater depths.

4.1.5. Facies 5: Hemipelagic/pelagic (>20–150 m?)

The pelagic/hemipelagic facies is dominated by planktonic foraminifera (e.g., *Globigerinoides*), delicate molluscs, small benthic foraminifera (*Textularia* sp.), abundant micrite and minor terrigenous grains (e.g., quartz and rock fragments) that commonly fill cavities created by multigenerational bioerosion (Fig. 7E,B) or occur as centimetre-scale caps on the top surfaces of other, shallower facies (Fig. 7A,D). Finally, Fe–Mn precipitates, ranging from millimetre- to centimetre-scale bulbous crusts (in the case of the Huon Gulf) are common on the outer surfaces of samples.

While it is difficult to define precisely the paleobathymetry of the microbial and hemipelagic/pelagic facies, stratigraphic relationships suggest they were deposited after the deep fore-reef slope coralline

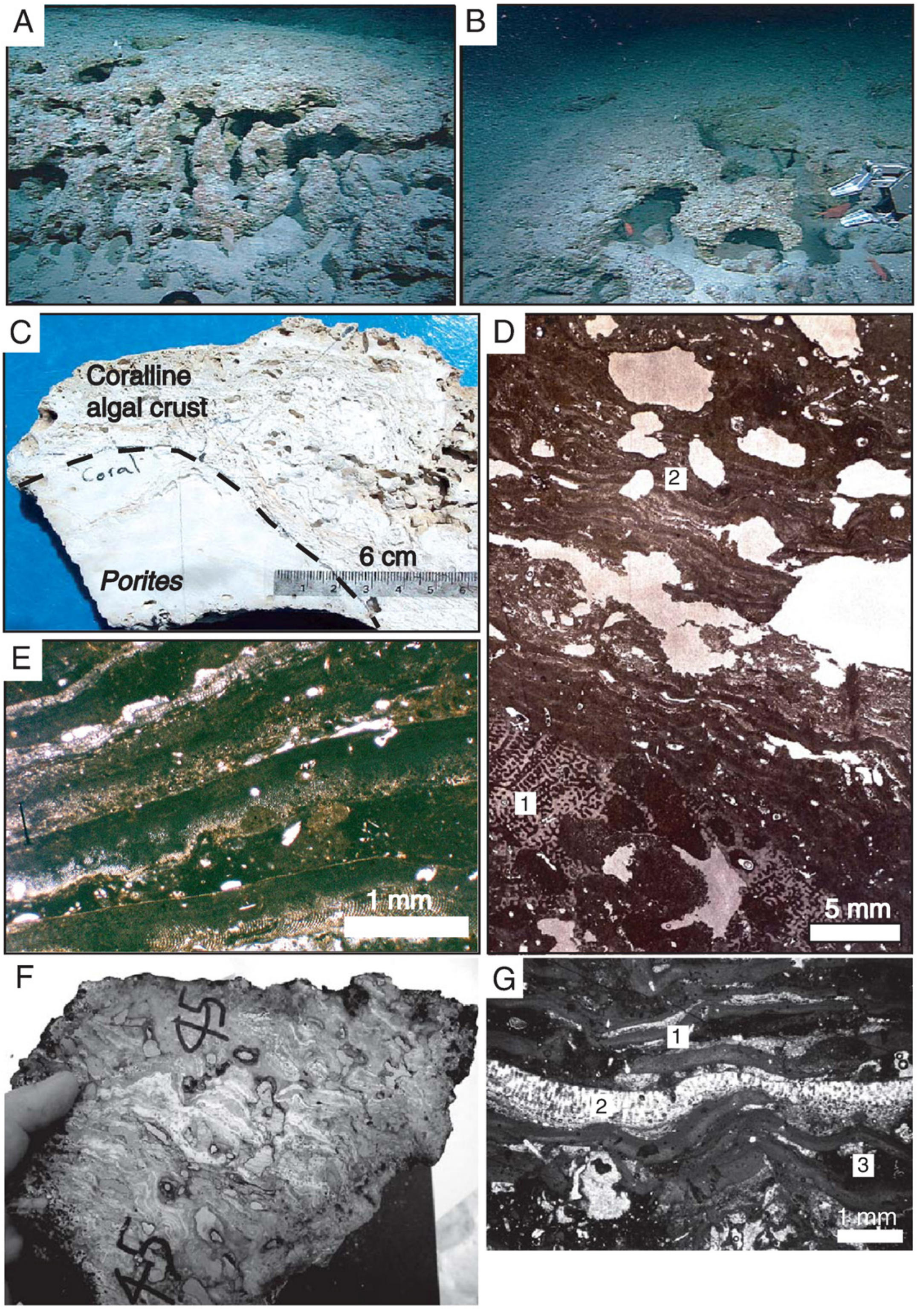

Fig. 6. Sedimentary facies deposited in deep fore-reef slope settings (Facies 3: −60 to −120 m). (A–B) Outcrop photos showing the coralline algal-dominated crust or pavement on the reef crest of H1 (−150 m, Hawaii). (C) Shallow-water reef-building *Porites lobata*? with thick crusts of coralline algae (H1, −175 m, Hawaii). (D) Photomicrograph of deepening sequence from a coral, *Porites,* (1) to an open framework of thick algal crusts (2) (H1, −150 m, Hawaii) (E) Close up photomicrograph of thin layers of *Mesophyllum*, *Lithothamnion*, and *Peyssonnelia*, with encrusting foraminifera, bryozoans, and interlayered micrite (H1, −156 m, Hawaii). (F) Limestone composed of coralline algal and foraminiferal crusts (PIV, −642 m, PNG). (G) Photomicrograph of alternating thin crusts of nongeniculate algae dominated by a melobesioid assemblage (1), encrusting foraminifera (2) and micrite (3) (PII, −239 m, PNG) (after Webster et al., 2004a,c).

algal-foraminiferal facies. These relationships, combined with their textures and compositions, suggest deposition within mainly non-reefal, deep open platform settings (~>−120 to −150 m). This deposition added little to the stratigraphic thicknesses of the reefs, but these facies form important lithostratigraphic and chronostratigraphic horizons marking complete platform turn off and represent 'drowning unconformities' in the context of carbonate platform literature (e.g., Erlich et al., 1990).

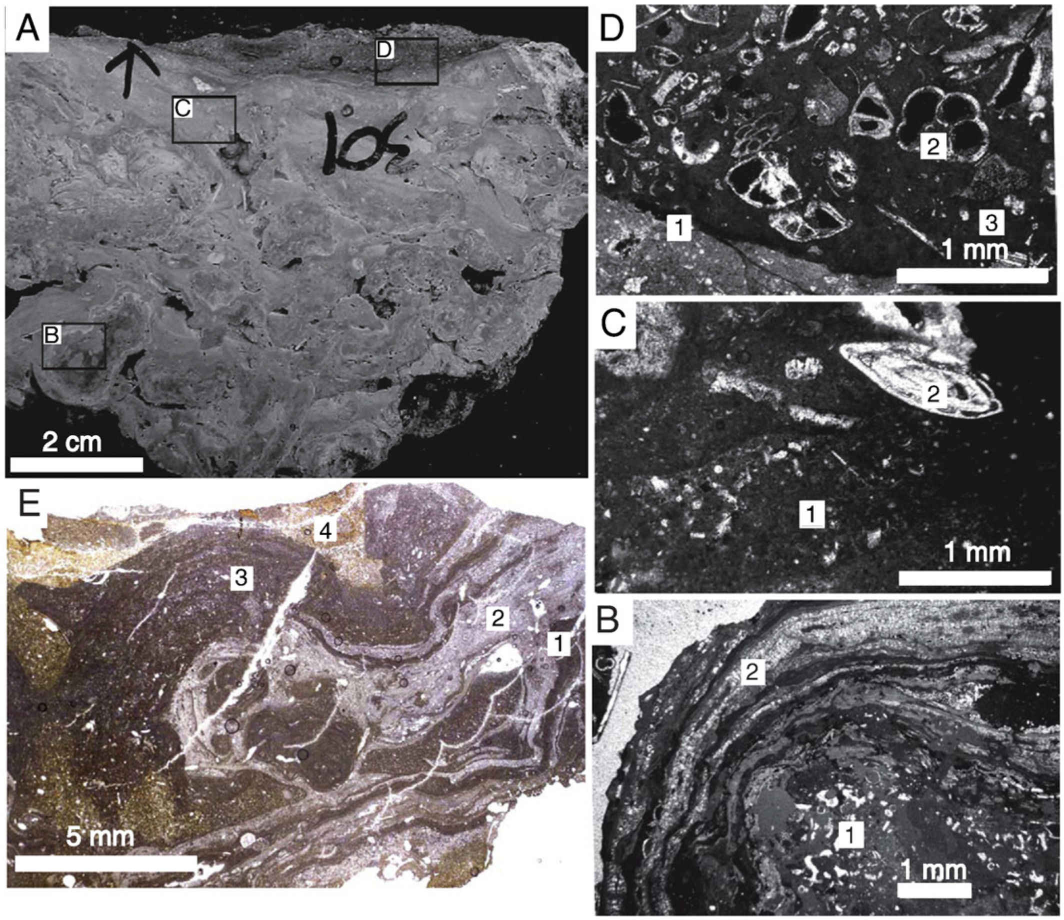

Fig. 7. Sedimentary facies deposited in deep fore-reef slope (Facies 3: −60 to −120 m) and deep-open platform settings (Facies 4, 5: >−120 to −150 m). (A) H and specimen showing an upward transition from coralline algal-foraminiferal nodules (B), to microbial micrite (C) and planktonic foraminifera (D) (PXIII, −2121 m, PNG). Rectangles outline the location of photomicrographs B–D from this sample. (B) Photomicrograph of the internal structure of a nodule with a bored and micritized coral nucleus (1), encrusted by concentric layers of coralline algae (e.g., *Lithothamnion*, *Mesophyllum* sp.) (2) and acervulinid foraminifera (3). (C) Photomicrograph showing the overlying clotted and peloidal microbial carbonate (1) with large benthic foraminifera (*Heterostegina depressa*) (2). (D) Photomicrograph showing the sharp contact (1) between the microbial carbonate and the overlying planktonic foraminifera limestone composed of planktonic foraminifera (2) and terrigenous grains (3). (E) Photomicrograph showing crusts of *Mesophyllum, Lithothamnion* (1), and acervulinid foraminifera (2) overlain by microbial carbonate with stromatolitic structure (3) later bored and filled by hemipelagic sediments (4) (H2, −444 m, Hawaii) (after Webster et al., 2004a,c).

4.2. Sedimentary signature of reef drowning

The five main facies and four paleoenvironmental settings are summarized in Fig. 8A. This figure represents an idealized, yet realistic, spatial and temporal paleoenvironmental scheme that fits both the Huon Gulf and Hawaiian drowned reefs (after Webster et al., 2004c). We use this framework to describe and interpret the distinct facies transitions recorded in the samples as evidence of reef and platform drowning associated with relative sea-level rise, reduced light, and changing water quality.

A major finding of our review of sedimentary data from the Huon Gulf and Hawaii is that coral reef drowning in rapidly subsiding settings is characterized by a distinct sequence of biological and sedimentary changes. Fig. 8B shows the generalized drowning sequence recorded on the tops of the drowned reefs. The sequence begins with the transition from: (1) shallow coral reef facies (shallow corals and mastophoroid algal crusts), to (2) intermediate coralgal facies (deeper-water corals, intermediate algal crusts or nodules), (3) deep fore-reef coralline algal facies (deep-water algal crusts or nodules), (4) microbial sediments and crusts, and finally (5) hemipelagic/pelagic sedimentation, multigenerational bioerosion and Fe–Mn crust development.

Although not involving identical biological changes, similar sedimentary sequences (i.e., deep-water facies overlying shallow-water facies) have been observed in ancient carbonate platforms (e.g., Schlager, 1981; Erlich et al., 1990) and used as evidence for platform drowning. However, our understanding of the mechanics of platform drowning is problematic, as it may reflect a real drowning brought about by a dramatic increase in the rate of relative sea-level rise and/or a decrease in the ability of the platform to produce carbonate.

Precise ^{14}C and U/Th dating of successive Huon and Hawaii drowned reefs allows us to better constrain the primary factors controlling reef and platform drowning. We argue that the observed biological changes and sedimentary sequences encapsulate a distinct signature of abrupt eustatic sea-level rise and coral reef drowning during major deglaciations and interstadial events, followed by a more gradual deepening and ultimately complete platform turn-off associated with continued relative sea-level rise (subsidence and eustatic rise), decreased light, and changes in water quality.

5. Timing of reef drowning and abrupt sea-level rise

5.1. Drowning during major deglaciations and interstadials

All available chronological (U-series, ^{14}C, Fe–Mn crust) ages for the Huon Gulf and Hawaiian reefs are plotted versus depth relative to present sea-level in Fig. 9. The Fe–Mn chronometer (Manheim and Lane-Bostwick, 1988) used in this study is the most accurate non-radiometric technique for determining growth rates of ferromanganese samples that have relatively low cobalt concentrations (Frank

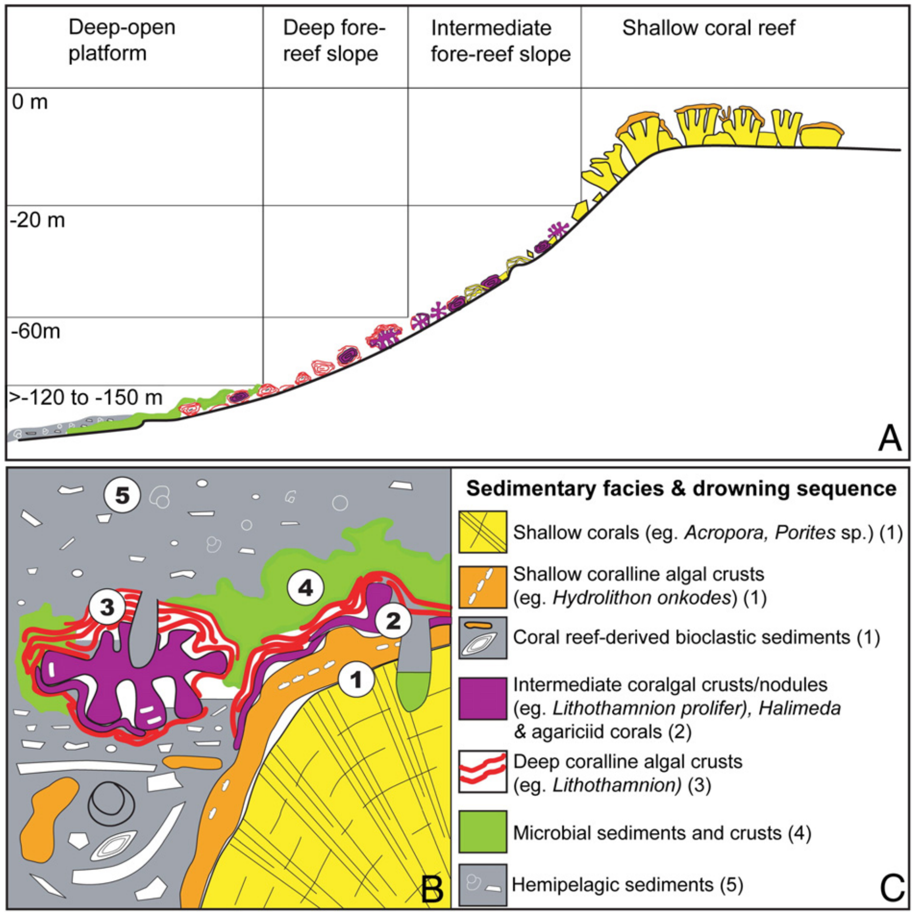

Fig. 8. (A) Generalized sedimentary facies model for the drowned Huon Gulf and Hawaiian reefs. (B) Generalized model showing the sequence of biological and sedimentary changes that result from reefs drowning on rapidly subsiding margins. Numbers indicate the sequence of distinctive sedimentary facies comprising the complete drowning signature. (C) Key to facies in drowning sequence.

et al., 1999). However, this technique is not without limitations (Table 1 for details) and thus the Huon Gulf Fe–Mn crust data must be considered as semi-quantitative, minimum ages. Taken together, the chronologic data support the concept of reef drowning in response to rapid eustatic sea-level rise, but also reflect differences between the Huon Gulf and Hawaiian tectonic settings (i.e., constant vs. flexural subsidence). For example, the age versus depth relationship in Hawaii is linear, due to steady rates of subsidence through time, whereas the Huon Gulf age versus depth distribution is nonlinear reflecting the steady increase in subsidence rates experienced by the reefs as they migrated towards the subduction load with time (Fig. 9 – dashed lines).

A single U/Th age from PXII (−2000 m) in the Huon Gulf of 348 ± 10 ka suggests drowning due to rapid sea-level rise associated with major deglaciation during the transition from MIS10 to MIS9 (or termination IV) (Galewsky et al., 1996) (Fig. 9). While the Fe–Mn crust data lack the precision needed to confirm this age they do suggest (with one exception) that reef PXII is at least older than 386 ka. Similarly, the Fe–Mn crust data cannot constrain the drowning ages of reefs PX, PVIII and PIV to specific eustatic events, but are broadly consistent with the age versus depth relationships expected from the variable flexural subsidence reported by Wallace (2002) and Webster et al. (2004b). Galewsky et al. (1996; 1998) identified four major reefs in the Huon Gulf that they interpreted as having drowned during as many major deglaciations. However, the more recent observations and numerical modeling data (Webster et al., 2004b) for the Huon Gulf indicate a more complex drowning history, with at least 14 distinct reefs and pinnacles, along with numerous smaller terraces within individual, multigenerational reefs (Fig. 2).

Five reliable U/Th coral ages and two ^{14}C-AMS ages (Riker-Coleman et al., 2004) indicate the PII (241 m) reef drowned at 57–67.4 ka, with later deep-water algal crust deposition at 35–43 ka. The timing of reef drowning coincides with a known period of rapid climate change (MIS4 to MIS3 transition) recorded in ice cores (Dansgaard–Oeschger event 17, Grootes et al., 1993; Sachs and Lehman, 1999), marine sediments (Heinrich event 6, Heinrich, 1988; Hemming et al., 2000) and an associated sea-level rise recorded directly in raised coral terraces in the nearby Huon Peninsula (Yokoyama et al., 2001; Chappell, 2002). These ages, when combined with bathymetry, sedimentary and numerical modeling data (Riker-Coleman et al., 2004; Webster et al., 2004b) are consistent with drowning during periods of rapid eustatic sea-level rise associated with higher frequency, smaller amplitude, interstadials events, in addition to major deglaciations. Further, the multigenerational features (i.e., multiple terrace levels) observed in some of the Huon Gulf and Hawaiian reefs (Figs. 2 and 3) may also owe their origin to repeated growth and demise during these interstadial/stadial events. However, currently there are no age data to confirm this.

Significantly more ^{14}C and U-series data are available for Hawaii than for the Huon Gulf (Fig. 9). These data and subsequent numerical modeling are consistent with the general pattern of reef drowning during major deglaciations, but this can only be firmly established for H2 and H1. The larger and more precise chronologic data set indicates that these reefs likely drowned during the penultimate (termination II) and last deglaciation (termination I) respectively. Further, data from H1 indicates that distinct, suborbital “jumps” in eustatic sea-level called meltwater pulse events (MWP) may be the primary cause of reef drowning during the deglaciations (Fig. 10).

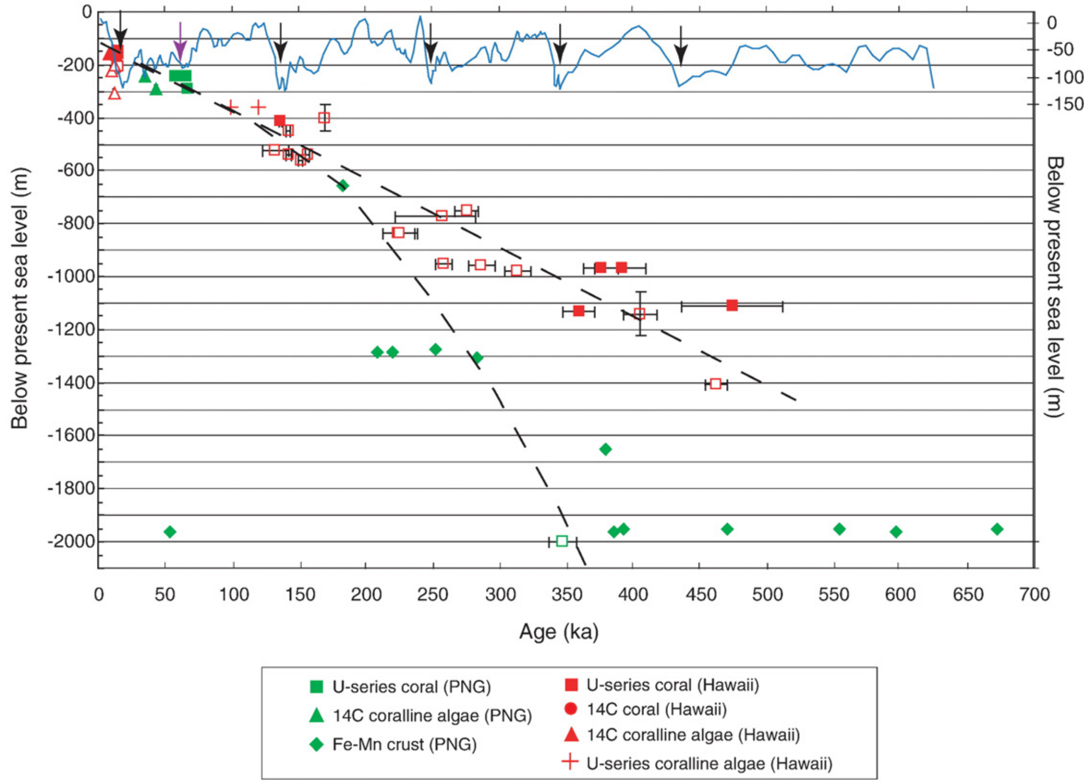

Fig. 9. Chronological age vs. depth data for PNG and Hawaii. Eustatic sea-level (after Imbrie et al., 1984; Lea et al., 2002) is shown as well as periods of abrupt sea-level rise and reef drowning during major glacial terminations (black arrows) and interstadials (purple arrow). All ages represent calendar years (ages data after Szabo and Moore, 1986; Ludwig et al., 1991; Jones, 1995; Moore and Chadwick, 1995; Galewsky et al., 1996; Riker-Coleman et al., 2004; Webster et al., 2004a; Riker-Coleman et al., 2005). Filled symbols represent samples collected in-situ from the tops of the reefs by ROV or submarine. Open symbols represent samples of uncertain spatial context (i.e., dredged or collected as loose talus on the slope). The horizontal line through the symbols represents age uncertainties for ^{14}C and U-series data. Symbols with no horizontal line represent age errors less than the width of the symbol: for Fe–Mn crust the cumulative precision is 3% based on the precision of the analytical data for Mn, Fe and Co used in the growth-rate calculations (see footnote to Table 1). For scaling purposes two Fe–Mn crust ages (1095 ka, 1384 ka) are not shown. Dashed lines represent the general subsidence trends for Hawaii (constant rate, 2.6 m/ka – Ludwig et al., 1991) and PNG (variable, flexurally driven – Webster et al., 2004b). (For interpretation of the references to colour in this figure legend, the reader is referred to the web version of this article.)

5.2. Drowning during the last two deglaciations – Hawaiian H2 and H1 case study

Nine U-series coral and two coralline algal ages have been reported for H2 and range between 170 and 99 ka. The youngest ages, 122±5 ka and 99±4 ka, come from coralline algal samples recovered from −360 m by Szabo and Moore (1986). However, it is difficult to assess the reliability of these ages given that coralline algae are susceptible to open-system behavior. Ludwig et al. (1991) published a single coral age of 133±10 ka for H2 but this was from loose material from the base of the fore-reef slope. Similarly, a coral age of 170 ka for H2 was reported from a dredge sample on the eastern side of Hawaii but its precise depth and stratigraphic position are unknown (Moore and Chadwick, 1995). More recently, Riker-Coleman et al. (2005) generated six reliable U/Th coral ages for H2 that range from 156–136 ka. These ages (and sedimentary facies) suggest that H2 is at least 156±2 ka but more importantly the youngest coral sample collected in-situ from the top of the reef (−412 m) implies that reef drowning and abrupt sea-level rise occurred at ~136±0.85 ka, consistent with rapid sea-level rise during the penultimate deglaciation (Esat et al., 1999; Gallup et al., 2002). Further, Riker-Coleman et al. (2005) argue that these data are consistent with Milankovitch theory which predicts that rapid sea-level rise during the glacial terminations is preceded by rising insolation (Fig. 10A).

Significantly more age data constrain the drowning of HI (Fig. 10C). Webster et al. (2004a) reported twenty-four ^{14}C and U/Th coral and algal ages from H1. Six reliable U/Th in-situ coral ages (15.2–14.7 ka) come from the shallow coral reef facies at the top of HI, while seven ^{14}C ages (14.6–8.3 ka) come from the overlying deep-water coralline algal crust facies. These data are consistent with shallow coral reef drowning at ~14.7 ka, synchronous with MWP-1A, followed by more deepening with continued eustatic sea-level rise and subsidence (Fig. 10A,C). There is considerable controversy concerning the precise timing and amplitude of MWP-1A (Weaver et al., 2003; Liu and Milliman, 2004). This uncertainty has important implications because MWP-1A, based on its timing at ~14 ka (Fairbanks, 1989; Bard et al., 1996), has been directly linked to catastrophic ice sheet collapse, subsequent disruption of ocean circulation, and global cooling (Bard et al., 1996). Others place the event earlier at ~14.7 ka, and argue that rather than driving a slow down of ocean circulation, MWP1A is synchronous with a major abrupt global warming (Bolling/Allerod) (Kienast et al., 2003; Webster et al., 2004a). Future work will focus on dating the shallower reef features around Hawaii (i.e., Fig. 3D) that probably grew and drowned during subsequent abrupt, but poorly constrained events (i.e., MWP 1B?, Fig. 10C) as well as precise dating of each stage of the sedimentary signature of reef drowning depicted in Figs. 8A and 11.

5.3. Sedimentary model of coral reef drowning on rapidly subsiding margins

Summarizing all available sedimentological and chronological data, we define five distinct and predictable stages of reef and platform drowning in response to abrupt eustatic sea-level rise and rapid subsidence. These stages are shown in Figs. 8 and 11 and summarized below.

Table 1
Growth rate and age determination for the Huon Gulf Fe–Mn crust samples

Sample #	Water depth (m)	Platform #	Fe[a] (%)	Mn[a] (%)	Co[a] (%)	GR[b] (mm/Ma)	Age[c] (ka)	Age[d] (ka)
Huon-32A	−655	PIV	11.7	15.6	0.0452	43.79	**183**	228
Huon-167A	−1275	PVIII	21.5	14.6	0.1664	7.90	**253**	633
Huon-161A	−1283	PVIII	20.3	13.1	0.1370	9.55	**209**	314
Huon-181A	−1287	PVIII	19.7	13.9	0.1118	13.55	**221**	295
Huon-156A	−1305	PVIII	21.2	13.1	0.1324	10.56	**284**	473
Huon-216A	−1653	PXI	19.5	13.3	0.1507	7.90	**380**	633
Huon-146A	−1950	PXII	18.5	17.3	0.1102	15.53	**471**	564
Huon-146B	−1950	PXII	19.8	16.6	0.0675	35.98	–	–
Huon-146C	−1950	PXII	25.7	13.4	0.1024	20.30	**555**	705
Huon-146D	−1950	PXII	21.4	14.9	0.0640	39.08	–	–
Huon-140A	−1953	PXII	19.5	15.6	0.1216	12.69	**394**	473
Huon-143A	−1953	PXII	16.7	17.3	0.0781	25.28	**673**	989
Huon-149A	−1960	PXII	20.8	15.8	0.1433	10.35	**386**	773
Huon-150A	−1960	PXII	19.7	20.0	0.0771	33.45	**598**	737
Huon-150B	−1960	PXII	13.9	24.6	0.0602	48.14	–	–
Huon-148A	−1961	PXII	22.7	14.7	0.1031	18.63	**54**	81
Huon-152A	−1963	PXII	16.4	17.0	0.0997	16.28	**1095**	1410
Huon-152B	−1963	PXII	12.7	21.6	0.0687	31.73	–	–
Huon-152C	−1963	PXII	13.5	21.1	0.0733	28.90	**1384**	1384

[a]Manganese and iron contents of ferromanganese crusts were determined by XRF and cobalt contents by ICP-MS.
[b]Growth rate determined from Manheim and Lane-Bostwick (1988) ($GR=0.68/(Co^*)^{1.67}$; $Co^*=Co$ wt.% • 50/Mn wt.%+Fe wt.%).
[c]Age determined by dividing the mean crust thickness by the GR (Fig. 9). This provides a minimum age of the crust because it does not account for possible growth or erosional hiatuses in the crusts, although these are probably minor in such young crusts. In thin crusts, such as those analyzed here, the crust ages are very sensitive to the crust thickness used in the calculations, and average crust thicknesses versus maximum crust thicknesses can give significantly different results. The crust thicknesses from a single sample can vary by up to 100%, or more. If there was a depression in the substrate that was filled in by ferromanganese oxides, that part of the crust can be much thicker than crust found elsewhere on the substrate. Thus, either the mean crust thickness or the [d]maximum crust thickness can be used to calculate crust ages. The mechanisms of crust growth are not known well enough to determine whether the thicker part of the crust (i.e., in the example just given) formed over a longer time period or grew faster in the depression during early crust growth. Detailed chemical analysis could distinguish between those two possibilities but was beyond the scope of this work. Also, on a broader scale, it is not known how representative the crust thickness of samples recovered by an ROV are with respect to the larger population of crusts over an entire reef.

5.3.1. Stage 1 – Shallow coral reef growth

Shallow coral reef facies dominate the final stages of the glacial maxima and the earliest parts of the deglaciations. During these periods the reef is able to keep pace with eustatic sea-level rise (and subsidence) but drowns following an abrupt eustatic rise in sea-level, perhaps caused by a meltwater pulse event. For the well-dated H1, this occurred about 5 ka after the start of the deglaciation at ~19–20 ka. By ~14–15 ka, all significant vertical reef accretion ceased as paleowater depths over the reef crest rose above the critical 30 m (Grigg and Epp, 1989) within less than 300–500 yrs (Fairbanks, 1989; Hanebuth et al., 2000).

5.3.2. Stage 2 – Intermediate coralgal growth

The period following the meltwater pulse and drowning of the shallow reefs is marked by a shift to an intermediate fore-reef slope setting in 20–60 m of water, characterized by coralline algae nodules and/or crusts with associated thin foliaceous corals. Samples of this facies have not been directly dated but it is probably established immediately after the meltwater pulse.

5.3.3. Stage 3 – Deep water coralline algal growth

Continued eustatic sea-level rise and subsidence (see grey subsidence path, Fig. 11), caused paleowater depths over the “reef crest” to exceed 60 m. In these deep fore-reef slope settings, coralline algae facies consisting of either crusts or nodules dominated until paleowater depths reached ~>120 m and lower light conditions prevailed. In Hawaii, the data suggest that this facies was deposited 1–4 ka after MWP1A and H1 reef drowning, while in the Huon Gulf deposition occurred ~14–22 ka after Heinrich 6 and PII reef drowning.

5.3.4. Stage 4 – Microbial carbonate accretion

Microbial carbonate sedimentation occurred after deepwater coralline algal deposition with continued relative sea-level rise. However, depth and light may not have been the only factors controlling the timing and occurrence of this facies. During major deglaciations greater upwelling of deep, nutrient-rich waters may occur (Brachert and Dullo, 2001; Cabioch et al., 2006). This can cause a significant increase in nutrient supply, particularly around volcanic islands, and combined with reduced terrigenous sediment flux, may allow microbialites to flourish in deep, fore-reef slope and platform settings (Camoin et al., 2006). The absolute timing of this facies is not constrained in Hawaii and the Huon Gulf but data from similar microbialite deposits off Tahiti and the Marquesas (Camoin et al., 2006) indicate that they are 1.6–8.4 ka younger than the underlying shallow coral reef facies.

5.3.5. Stage 5 – Hemipelagic/pelagic sedimentation and Fe–Mn precipitation

The final stage in this sequence is marked by hemipelagic/pelagic sedimentation, intense boring and infilling as well as Fe–Mn precipitation. This represents complete platform “turn-off” as the drowned reefs subsided beneath the photic zone and continued downwards until they reached their current depths.

6. Internal stratigraphic succession

6.1. Conceptual framework for numerical modeling

Numerical modeling by Galewsky (1998) and Wallace (2002) focused on growing and drowning the reefs in the Huon Gulf. More recently, Webster et al. (2004b) extended these efforts by trying to predict the specific timing of reef turn on and drowning as well as brief subaerial exposure and drowning events within the evolution of each reef. More detailed numerical models (constrained by observational data) were constructed for the Hawaiian reefs (Webster et al., 2007) allowing a detailed assessment of the internal stratigraphic and sedimentary facies succession within H2 and H1.

Conceptually, the initiation, growth and demise of coral reefs on rapidly subsiding margins is represented in Fig. 12. This figure shows the relationships between subsidence of the basement, eustatic sea-level changes, reef growth and subsequent changes in accommodation space available for platform sedimentation. Depending on the rate and magnitude of these parameters and the reef response, the platform experiences repeated periods of sustained shallow and deep-water accretion, brief subaerial exposure, and drowning events. In this simplistic example, the platform margin records these different stages, forming a complex ‘layer cake’ stratigraphic succession composed of shallow to deep reef and platform packages, separated by repeated subaerial exposure horizons and drowning unconformities.

The well preserved H2 and H1 reefs off NW Hawaii (Figs. 1 and 2) have been the focus of detailed modeling (Webster et al., 2007) for several reasons. First, the most extensive database of bathymetric, submersible, ROV observations, sedimentary facies and radiometric data is available for these reefs. Second, ^{14}C and U/Th age dating of these reefs indicate that they probably grew and certainly drowned during the last two interglacial–glacial cycles (Fig. 10). Third, several independent high-resolution eustatic sea-level curves (e.g., Lambeck and Chappell, 2001; Lea et al., 2002) for the Pacific Ocean are available as model inputs that cover this 250 ka period. Fourth, in contrast to the Huon Gulf, the slope angle and depth of the basement volcanic substrate forming the original growth surface can be reasonably estimated. Fifth, and again unlike the Huon Gulf, the subsidence rate (~2–3 m/ka) for Hawaii is relatively constant over this time scale (Moore and Campbell, 1987; Ludwig et al., 1991; Moore et al., 1996)

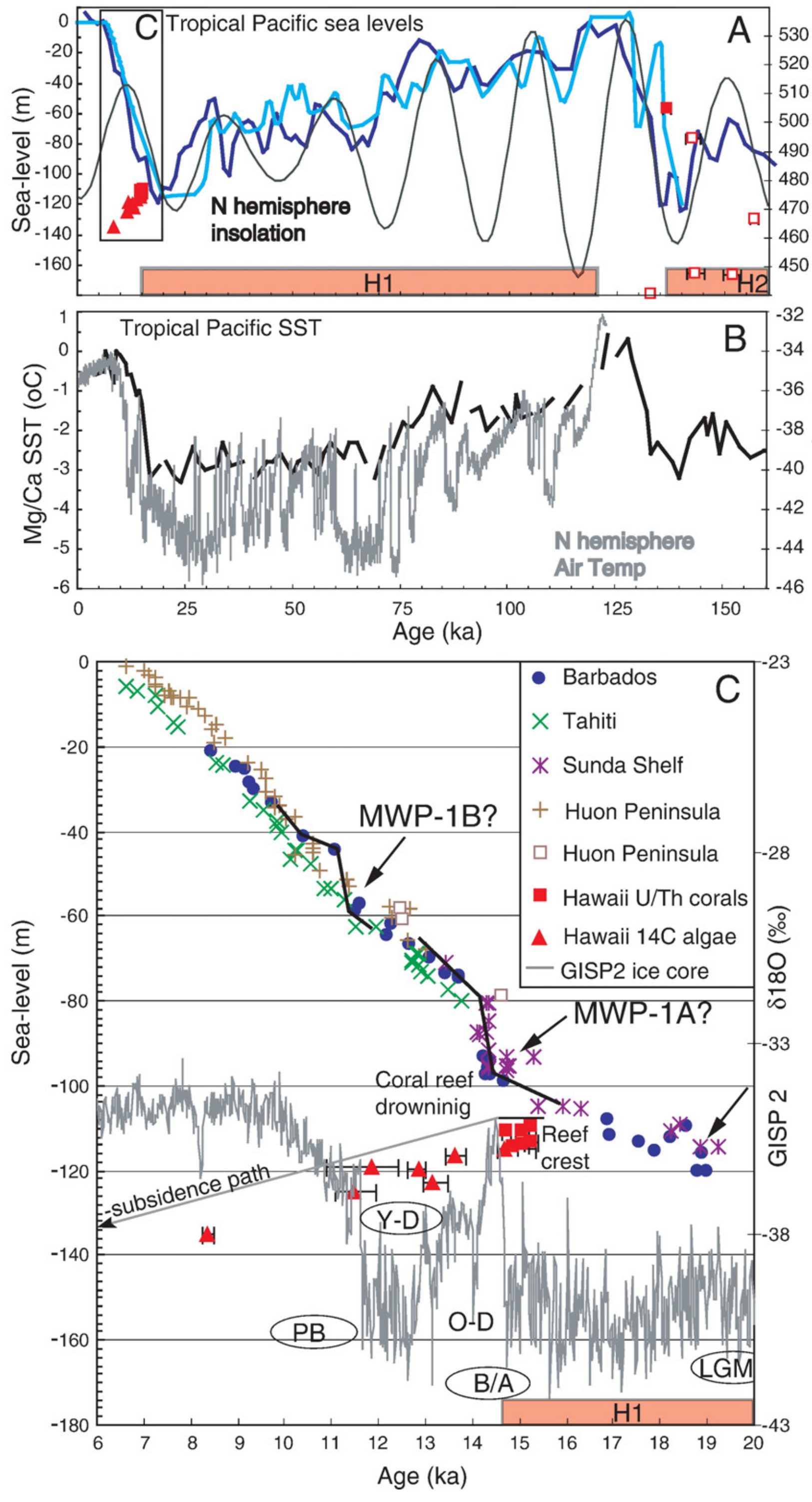

Fig. 10. Drowning history of the −400 m (H2) and −150 m (H1) reefs around Hawaii. (A) Eustatic sea-level change (light blue line – Lambeck and Chappell, 2001; dark blue line – Lea et al., 2002) and 60° N hemisphere June solar insolation (thin black line – Berger and Loutre, 1991) over the last 160 ka. Drowning ages and depths of H2 and H1 as defined by radiometric coral (red squares, U/Th) and coralline algal ages (red triangles, ^{14}C) that have been corrected for island subsidence (after Ludwig et al., 1991; Webster et al., 2004a; Riker-Coleman et al., 2005; Webster et al., 2007). Solid red symbols are in-situ samples from the reef crest while open squares were loose on the reef slope. Horizontal red bars give age ranges for the duration H2 and H1 reef growth based on observational and numerical modeling data (Webster et al., 2007). Rectangle C outlines H1 drowning expanded in Fig. 10C. (B) Sea surface temperature from the western tropical Pacific (black line – Lea et al., 2003) and the Greenland ice record (grey line – NGRIP) for the last 160 ka. (C) Drowning of −150 m reef (H1) during last deglaciation (after Webster et al., 2004a). Calibrated ^{14}C and U/Th ages from H1 are superimposed on relative sea-level records from Barbados, Tahiti, Huon Peninsula, and the Sunda Shelf. Original positions (adjusted for subsidence at 2.6 m/ka) of the H1 reef crest (and samples) before drowning. Filled red symbols represent in-situ coral and coralline algal samples collected from the reef crest. Space between the reef crest, subsidence pathway (grey line), and sea-level records approximates paleowater depth above reef crest during last deglaciation. Abrupt sea-level associated with MWP-1A may have drowned H1 and forced subsequent abrupt global scale cooling events (i.e., O–D = Older Dryas, Y = Younger Dryas) shown here in ice core data (grey line – GISP II). LGM = Last Glacial Maximum, B/A = Bølling–Allerod transition and PB = Preboeral. (For interpretation of the references to colour in this figure legend, the reader is referred to the web version of this article.)

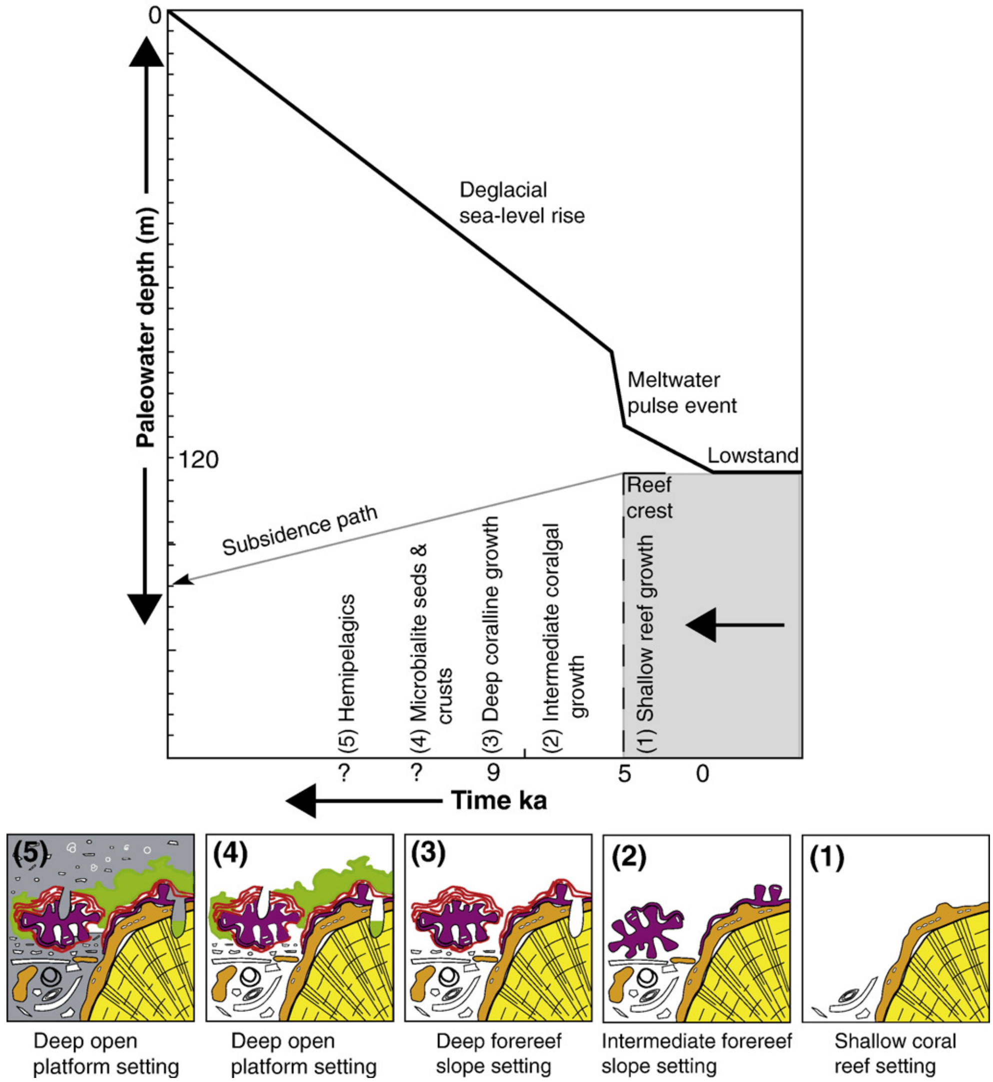

Fig. 11. Sedimentary model summarizing the five stages of reef drowning in response to abrupt eustatic sea-level rise and rapid subsidence The eustatic sea-level rise is based on the last deglaciation and incorporates an episodic "jump" or meltwater pulse of sea-level about 5 ka following the end of the glacial maximum. We use 2.6 m/ka (subsidence of Hawaii) to define the subsidence pathway of the reef crest through time and chronologic data from Webster et al. (2004a) for the *x*-axis. Sedimentary facies symbols are the same as those shown in Fig. 8 and see text for detailed explanation of each stage.

(i.e., Fig. 9). Finally, a plunge pool system east of Kohala (Fig. 14) has exposed a stratigraphic section through H7 (−968 to −926 m). Although not of the same age, samples and observations from this section can be used to support the complex growth history demonstrated by modeling H2 and H1 reef evolution.

6.2. H1, H2 modeling and H7 observational data

The "best case" modeling scenario indicates that growth of both H2 and H1 initiated growth during the relatively stable sea-levels associated with highstands in the early stages of MIS7 (222 ka) and MIS5 (126 ka) (see Fig. 13 for model inputs and outputs). This finding is consistent with the qualitative predictions of previous studies on the drowned reefs around Hawaii (e.g., Moore and Fornari, 1984; Ludwig et al., 1991). No observational data constrain the timing of initiation of H2 and H1, but data from H7 east of Kohala provides tentative support for the initiation of drowned reefs during highstands. ROV observations show a well exposed 40 m thick stratigraphic section through H7. Two reliable U/Th coral ages (*Leptastrea*, *Porites*) (Fig. 9) from the in-situ shallow coral reef facies growing directly on the basalt substrate at the base of this section (Fig. 14D,H) confirm that reef growth was initiated between 392 (±20/17.9) ka and 377 (±13/12) ka during the MIS11 highstand.

Modeling suggests that the reefs are likely to have long, complex growth histories and internal stratigraphies. For H2, a 143 m thick stratigraphic sequence developed over 90 ka with eight distinct shallow, coral reef dominated units (Fig. 13A). These units are separated by four subaerial horizons and three distinct drowning events (not including the final drowning), characterized by <5 m thick sequences of intermediate coralgal facies that formed during major MIS7 interstadials. H1 developed over a period of 90 ka, producing a 186 m thick stratigraphic sequence (Fig. 13B). Because of high frequency, suborbital sea-level fluctuations (Lea et al., 2002) during the last glacial cycle, eleven distinct shallow coral reef dominated units are separated by eight subaerial horizons and three brief (<10 ka) reef drowning events (not including the final drowning). Recent studies of raised Pleistocene coral reefs in Papua New Guinea (Chappell, 2002) and Barbados (Blanchon and Eisenhauer, 2001) also record short-term, polycyclic reef deposition in response to suborbital sea-level fluctuations.

Currently, there are no seismic or drilling data confirming the complex internal stratigraphies of H2 and H1. However, ROV observations of the H2 reef face show several alternating sections of coral-dominated and algal-dominated limestones. Further support for complex internal stratigraphy comes from H7 (Fig. 14). ROV sampling at the base and top of this section, combined with detailed

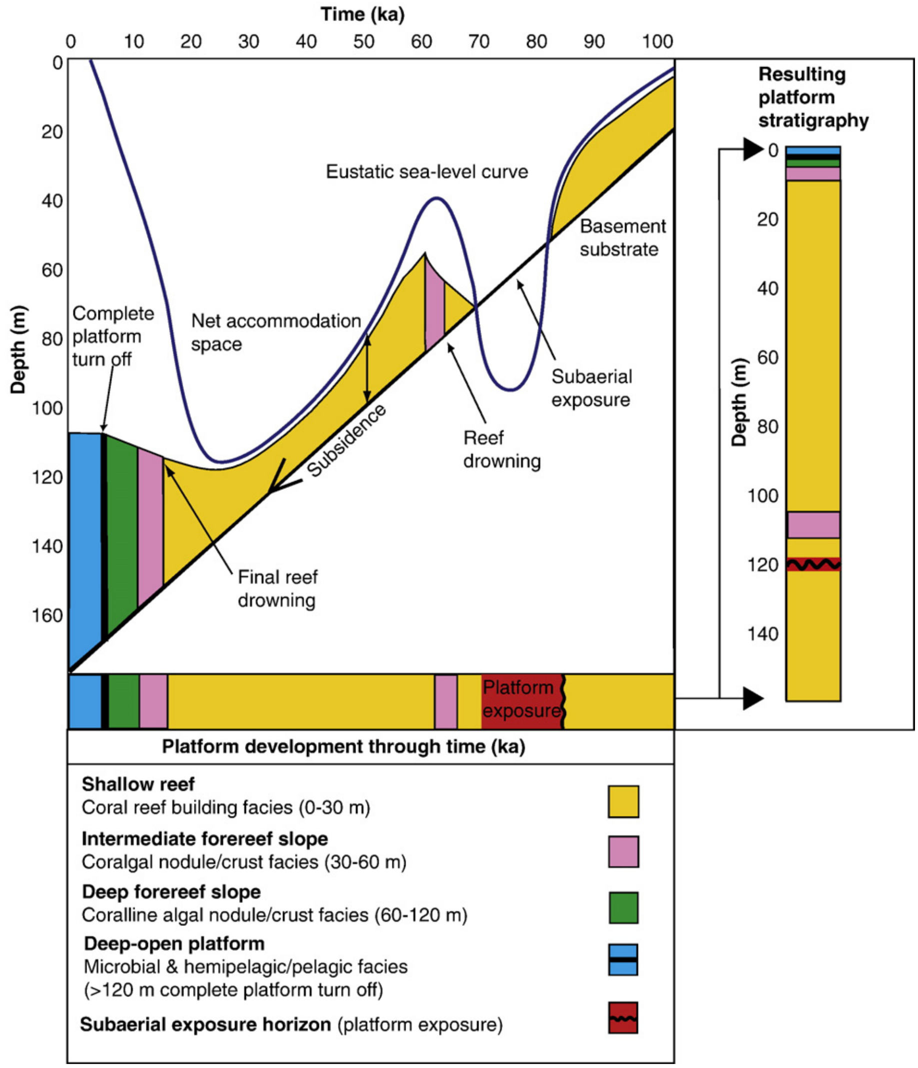

Fig. 12. Conceptual model of coral reef initiation, growth and demise over a hypothetical ~100 ka eustatic sea-level cycle on a rapidly subsiding margin. The basement substrate experiences constant subsidence of the order of 2–3 m/ka, roughly similar to the mean rate of sea-level fall from the highstand to the lowstand. Depending on the rate and amplitude of eustatic sea-level rise and reef response, the reef develops in a complex 'layer cake' or aggradational fashion, with several different reef packages preserved that are separated by brief subaerial exposure and/or drowning horizons. Fig. 13 shows our quantitative demonstration of the conceptual model with respect to our best case scenarios for H2 and H1 in Hawaii (after Webster et al., 2007).

observations, reveals at least six distinct reef units (Fig. 14B–H). These are characterized by different in-situ coral volumes and framework types that are separated in places by enigmatic planar, surfaces (Fig. 14G), perhaps representing either thick coralline algal crusts and/or subaerial exposures surfaces. These observations provide tantalizing evidence of alternating shallow reef growth, subaerial exposure and possible reef-drowning horizons, similar to the complex stratigraphic successions predicted by the numerical models of H2 and H1 (Fig. 12) (Webster et al., 2007).

Final reef drowning in the model is defined by the timing of the final shift from shallow coral reef to intermediate fore-reef facies (>30 m). This transition is observed directly at the hand specimen scale but also at the outcrop scale in the exposed section through H7. Unit 5 to Unit 6 (Fig. 14F) shows a marked transition from robust branching and submassive coral frameworks to thin encrusting-foliaceous coral frameworks consisting of *Leptoseris hawaiiensis*? intergrown with and encrusted by intermediate coralline algae (e.g., *Mesophyllum erubescens*) (Fig. 5B). For H2 and H1, our 'best case' scenario indicates that final reef drowning occurred between 133–134 ka and 12–14 ka respectively, consistent with chronologic data (Figs. 9 and 10A,C). The close match between model results and observational data for H2 and H1 is compelling given that the model (Webster et al., 2007) is not 'forced' by actual drowning ages, but rather generates these results independently from the model parameters.

7. Implications for drilling, new records of sea-level, climate change and reef response of the last six glacial cycles

Numerical modeling and observational data from Hawaii (Webster et al., 2007) and the Huon Gulf (Galewsky, 1998; Webster et al., 2004b) indicate that the internal stratigraphy of reefs growing on rapidly subsiding margins is highly sensitive to sea-level and climate change over the last 500 ka. We argue that the predicted stratigraphic successions combined with extensive observational data, provide a firm template with which to conduct drilling operations in Hawaii so these hypotheses can be tested as well as generating new sea-level and climate records.

The numerical model for Hawaii predicts the number of shallow coral reef units and their age vs. depth relationships. The units are separated by subaerial exposure horizons as well as deeper water coralgal units that mark brief reef drowning as a result of high frequency eustatic sea-level fluctuations. As a direct result of Hawaii's rapid but constant subsidence, a thick (100–200 m) expanded sequence of shallow coral reef-dominated

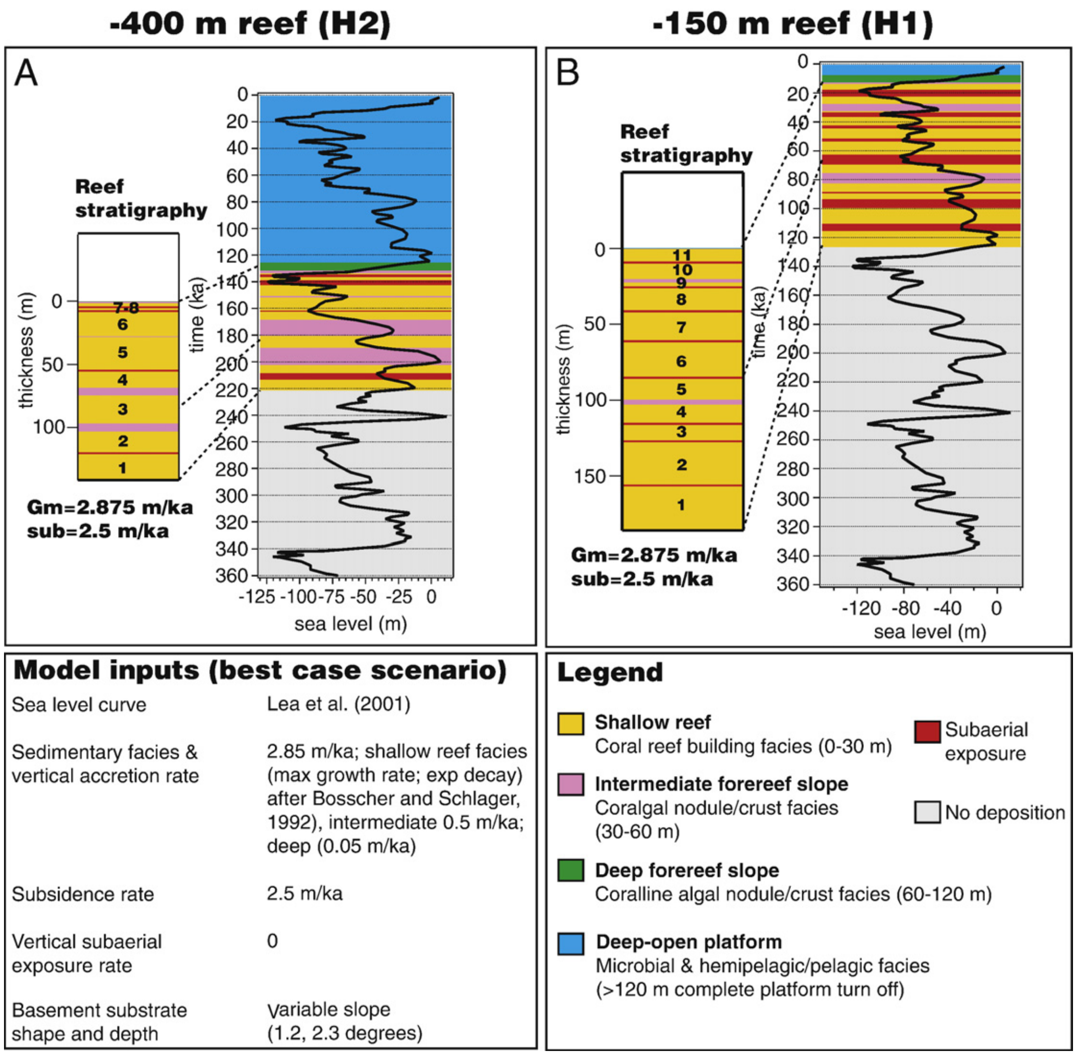

Fig. 13. Model outputs showing predicted internal reef evolution and stratigraphy of H2 (A) and H1 (B) around Hawaii based on our 'best case' model scenario (after Webster et al., 2007). Gm represents the maximum coral growth rate and sub the subsidence rate used in the model.

facies are preserved in both H2 and H1 that span important periods in Earth's climate history (Fig. 13A,B). These are either unavailable or in a highly condensed form on stable (e.g., Great Barrier Reef, Webster and Davies, 2003) and uplifted margins (e.g., PNG, Lambeck and Chappell, 2001) due to a lack of continual creation of accommodation space and unfavorable shelf morphology (e.g., Tahiti, Camoin et al., 2007). Specifically, this model shows that the reefs grew (albeit episodically) into, during, and out of most (~90 ka) of the last two glacial cycles.

Drilling through H2 and H1 will generate a new and unique record of sea-level and associated climate variability during several, controversial and poorly understood periods: the penultimate glaciation (MIS6) and deglaciation (MIS6-5), MIS5, MIS4, MIS3, MIS2 (i.e., LGM) and the last deglaciation (Lambeck and Chappell, 2001; Lambeck et al., 2002) (Fig. 10). These data will directly constrain the timing, rate, and amplitude of sea-level variability (assuming known subsidence) allowing a definitive test of Milankovitch climate theory as well as an assessment of the controversial abrupt sea-level events (i.e., meltwater pulses) that occur on suborbital frequencies (Esat et al., 1999; Chappell, 2002; Thompson and Goldstein, 2005) in concert with climate events occurring in the extra-tropics (i.e., ice core temperature cycles – Dansgaard/Oeschger (D/O) Events, and related ice-rafted debris in North Atlantic sediment cores – Heinrich Events). Finally, a transect of cores through all ten Hawaiian drowned reefs would generate an unparalleled record of sea-level, climate variability and coral reef response over at least the last six glacial cycles (Fig. 15).

8. Conclusions

Based on a review of new and existing data from the drowned reefs in the Huon Gulf and Hawaii, we draw the following conclusions;

1. Fourteen drowned coral reefs have been identified in the Huon Gulf and twelve around Hawaii. Morphologically, the Huon Gulf reefs are more complex, with highly sinuous margins and a diverse suite of associated pinnacles and banks. This configuration closely mimics the morphology of the present Huon Gulf coastline, seaward islands and shoals, and demonstrates the role of original geology and basement topography in controlling reef development. This relationship is also illustrated in Hawaii where the onland slope may have influenced reef morphology (e.g., determining shape and width).
2. The reefs record evidence of primary growth features (e.g., raised reef crests, spurs and grooves, patch reefs, and lagoons) as well as of erosional processes. Evidence of localized mass wasting of the reef margins includes fracturing, platform incision, slumped decimeter blocks, and slope-ward debris. The timing and cause of this mass wasting is unknown.
3. The reefs are commonly multigenerational features, comprised of multiple terraces and benches. These features likely owe their origin to a complex history of growth, drowning, and minor backstepping in response to high frequency climate and sea-level events.

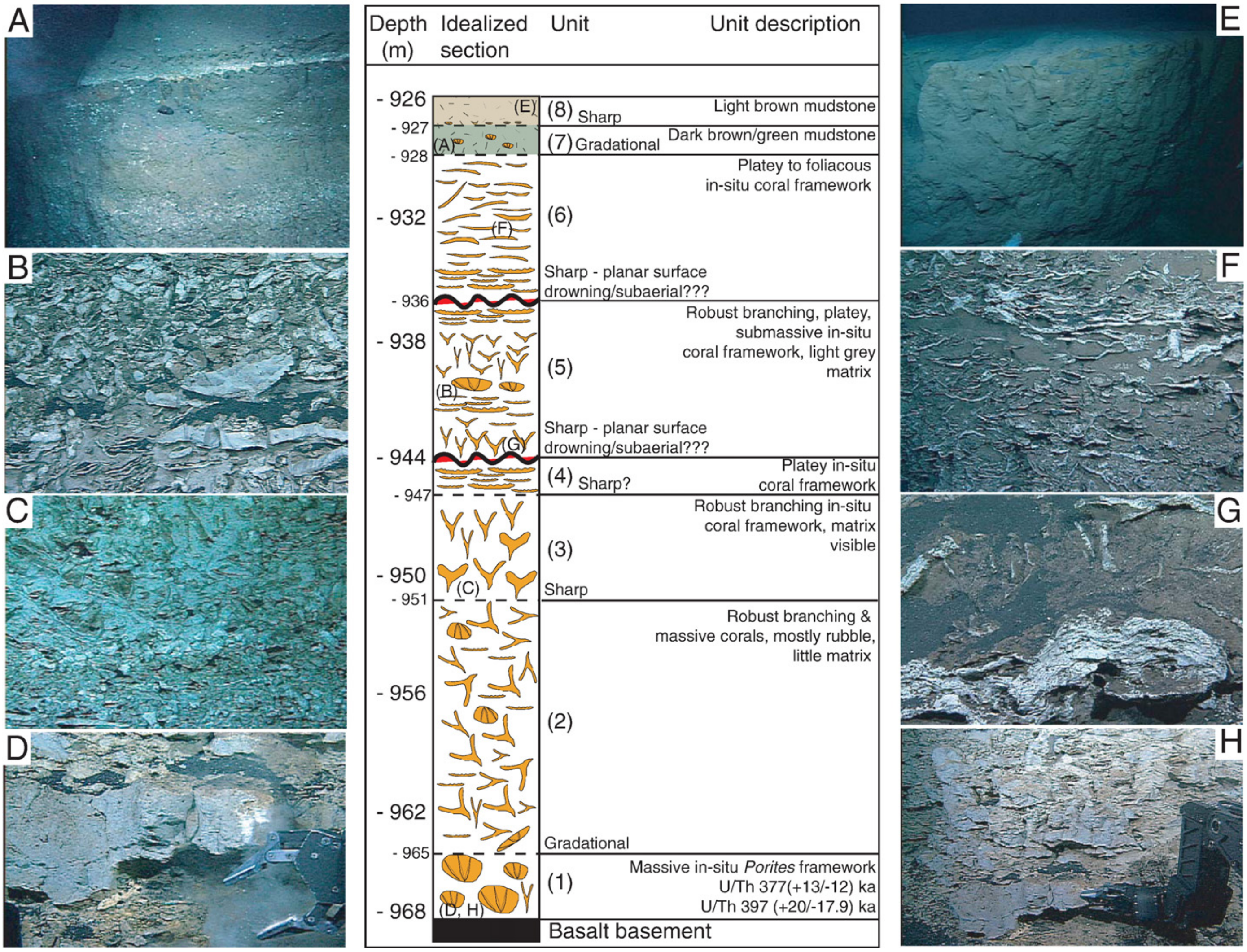

Fig. 14. Stratigraphic section through H7 (−950 m) off Kohala, NE Hawaii. (A) Outcrop photo showing the transition between Unit 6–8. Note the sharp contact defined by carbonate? debris between Units 7 and 8. (B) Outcrop photo showing in-situ platey and submassive coral framework from Unit 5. (C) Outcrop photo showing transition between Unit 2 and 3 characterized by coral rubble and in-situ robust branching coral framework respectively. (D, H) Outcrop photo showing Unit 1 dominated by in-situ massive *Porites lobata*? forming the shallow coral reef facies. U/Th age data indicates this unit was deposited during MIS11 (377–397 ka). (E) Outcrop photo showing light brown hemipelagic mudstone forming Unit 8 at the top of the section. (F) Outcrop photo showing the in-situ platey to foliaceous coral framework towards the top of Unit 6. This unit is characterized by thin overlapping agaricid corals (*Leptoseris, Pavona*) with inter-growing coralline algae (i.e., *Lithothamnion prolifer*) representing the intermediate, fore-reef slope facies. (G) Outcrop photo showing a sharp planar, surface separating Units 4 and 5.

4. Despite taxonomic and compositional differences, five generalized sedimentary facies (shallow coral reef, intermediate coralgal crust/nodule, coralline algal-foraminifera crust, microbial, hemipelagic/pelagic sediment) are common to both reef systems. They represent a range of paleoenvironments from shallow-reef to deep, open-platform settings.

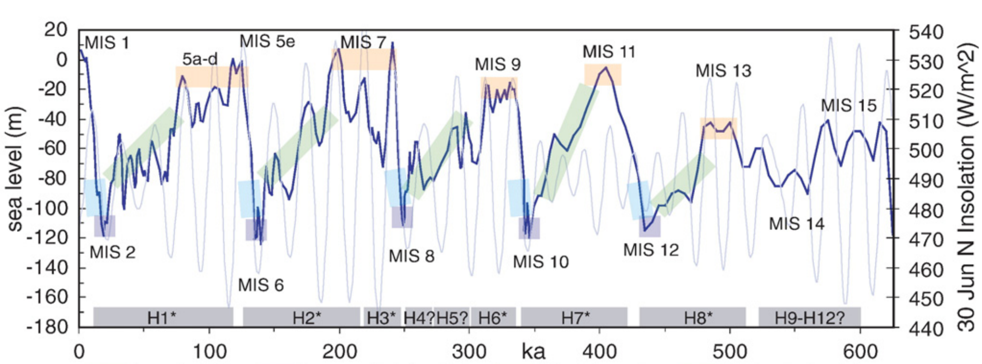

Fig. 15. Sea-level, climate and insolation history over the last 600 ka (Imbrie et al., 1984; Berger and Loutre, 1991; Lea et al., 2002). Observational and numerical modelling data indicate that the succession of drowned Hawaiian reefs (H1–H12) grew episodically over this period during different interglacial, interstadial/stadial, glacial maxima and deglacial intervals.

5. Coral reef drowning in rapidly subsiding settings is characterized by a distinct biological and sedimentary sequence. The occurrence and timing of this drowning signature is likely controlled by increasing paleowater depths, associated first with abrupt eustatic sea-level rise followed by decreasing light, decreasing sediment flux and increasing nutrients caused by continued eustatic sea-level rise and subsidence.
6. Chronological data (U-series, ^{14}C, Fe–Mn crusts) confirm that the reef systems have evolved over the last 500 ky. These data also suggest that they not only drown during major deglaciations, but also during distinct abrupt climate change events such as interstadials/stadial transitions (i.e., D/O 17, Heinrich 6) during the last glacial period and meltwater pulses (i.e., MWP-1A) during the last deglaciation. These findings confirm the sensitivity of reefs on rapidly subsiding margins to abrupt sea-level and climate change.
7. Observation and numerical stratigraphic modeling indicate that the reefs have had a long and complex growth history. Reefs H2 and H1 in Hawaii grew episodically for ~90 ka. Because of precessional (~20 ka) and higher frequency, suborbital eustatic sea-level fluctuations, each reef experienced repeated, but brief (<5–10 ka) drowning and subaerial exposure throughout its evolution. As a result, their internal stratigraphic succession is a complex layer-cake stratigraphy of many shallow coral reef units separated by either subaerial exposure horizons or thin intermediate depth coralgal units during brief drowning phases. These findings are consistent with ROV observations of H2 and H7.
8. We find that over precessional (20 ka) and sub-orbital timescales, the rate and amplitude of eustatic sea-level changes is critical in controlling initiation, growth, drowning or sub-aerial exposure, subsequent re-initiation, and final drowning. However, continued tectonic subsidence and basement substrate morphology influence broad-scale reef morphology and backstepping over longer time-scales (>100–500 ka).
9. Drilling of these structures, particularly in Hawaii, will likely yield greatly expanded stratigraphic sections compared with similar reefs on slowly subsiding, stable, and uplifted margins. Therefore, these reefs represent a unique archive of sea-level and climate changes, as well as coral reef response over the last six glacial cycles.

Acknowledgments

The work in PNG was funded by the US National Science Foundation grants OCE-9907153 to Silver and OCE-9907869 to Gallup. We also thank the captain and crew of the R/V *Melville* for their support during the cruise. For the work around Hawaii, we thank NOAA's Hawaiian Undersea Research Laboratory (HURL) for their work in the 1980s during the submersible dives that collected many samples used in the study. The most recent Hawaiian samples were collected during MBARI's expedition in 2001. The expedition, as well as the subsequent laboratory study of the samples by JMW and DAC was supported by the David and Lucile Packard Foundation through a grant to MBARI. We thank the captain and crew of the R/V *Western Flyer*, and the ROV *Tiburon* pilots for their outstanding work in collecting the samples.

References

Abbott, L.D., Silver, E.A., Galewsky, J., 1994a. Structural evolution of a modern arc-continent collision in Papua New Guinea. Tectonics 13 (5), 1007–1034.
Abbott, L.D., Silver, E.A., Thompson, P.R., Filweicz, M., Abdoerrias, S., Schneider, C., 1994b. Stratigraphic constraints on the development and timing of the arc-continent collision in northern Papua New Guinea. Journal of Sedimentary Research 64 (2), 169–183.
Abbott, L.D., Silver, E.A., Anderson, R.S., Smith, R., Ingle, J.C., Kling, S.A., Haig, D., Small, E., Galewsky, J., Sliter, W., 1997. Measurement of tectonic surface uplift rate in a young collisional mountain belt. Nature 385, 501–507.
Bard, E., Hamelin, B., Arnold, M., Montaggioni, L., Cabioch, G., Faure, G., Rougerie, F., 1996. Deglacial sea-level record from Tahiti corals and the timing of global meltwater discharge. Nature 382, 241–244.
Berger, A., Loutre, M.F., 1991. Insolation values for the climate of the last 10 million years. Quaternary Science Reviews 10 (4), 297–317.
Blanchon, P., Eisenhauer, A., 2001. Multi-stage reef development on Barbados during the Last Interglaciation. Quaternary Science Reviews 20 (10), 1093–1112.
Brachert, T.C., Dullo, W.C., 2001. Laminar micritic crusts and associated foreslope processes. Journal of Sedimentary Petrology 61 (3), 354–363.
Braga, J.C., Webster, J.M., Clague, D.A., Moore, J.G., Spalding, H., 2005. Very deep water coralline algae (Corallinales, Rhodophyta) off Hawaii. Phycologia 44 (Supplement) Abstract 12–13.
Cabioch, G., Camoin, G.F., Montaggioni, L.F., 1999. Postglacial growth history of a French Polynesian barrier reef tract, Tahiti, central Pacific. Sedimentology 46, 985–1000.
Cabioch, G., Camoin, G., Webb, G.E., Le Cornec, F., Garcia Molina, M., Pierre, C., Joachimski, M.M., 2006. Contribution of microbialites to the development of coral reefs during the last deglacial period: case study from Vanuatu (South-West Pacific). Sedimentary Geology 185 (3–4), 297–318.
Caccamise, D.J.I., Merrifield, M.A., Bevis, M., Foster, J., Firing, Y.L., Schenewerk, M.S., Taylor, F.W., Thomas, D.A., 2005. Sea level rise at Honolulu and Hilo, Hawaii: GPS estimates of differential land motion. Geophysical Research Letters 32 (L03607). doi:10.1029/2004GL021380.
Camoin, G., Cabioch, G., Eisenhauer, A., Braga, J.C., Hamelin, B., Lericolais, G., 2006. Environmental significance of microbialites in reef environments during the last deglaciation. Sedimentary Geology 185 (3–4), 277–295.
Camoin, G.F., Iryu, Y., McInroy, D.B., Scientists, E., 2007. Proceedings of the Integrated Ocean Drilling Program Volume 310 Expedition Reports TAHITI SEA LEVEL. Proceedings of the Integrated Ocean Drilling Program, vol. 310. doi:10.2204/iodp.proc.310.101.2007.
Chappell, J., 1974. Geology of coral terraces, Huon Peninsula, New Guinea: a study of Quaternary tectonic movements and sea-level changes. Geological Society of American Bulletin 85 (4), 553–570.
Chappell, J., 2002. Sea level changes forced ice breakouts in the Last Glacial cycle: new results from the coral terrraces. Quaternary Science Reviews 21 (10), 1229–1240.
Clague, D.A., Reynolds, J.R., Maher, N., Hatcher, G., Danforth, W., Gardner, J.V., 1998. High-resolution Simrad EM300 Multibeam surveys near the Hawaiian Islands: Canyons, reefs, and landslides,. Eos Transactions Fall Meeting Supplement. American Geophysical Union, San Francisco. F826 Abstract.
Davies, H.L., Honza, E., Tiffin, D.L., Lock, J., Okuda, Y., Keene, J.B., Murakami, F., Kisimoto, K., 1987a. Regional setting and structure of the western Solomon Sea. Geo-Marine Letters 7 (3), 153–160.
Davies, H.L., Lock, J., Tiffin, D.L., Honza, E., Okuda, Y., Murakami, F., Kisimoto, K., 1987b. Convergent tectonics in the Huon Peninsula region, Papua New Guinea. Geo-Marine Letters 7 (3), 143–152.
Davies, P.J., Braga, J.C., Lund, M., Webster, J.M., 2004. Holocene deep water algal buildups on the Eastern Australian shelf. Palaios 19 (6), 598.
Erlich, R.N., Barrett, S.F., Ju, G.B., 1990. Seismic and geologic characteristics of drowning events on carbonate platforms. AAPG Bulletin 74 (10), 1523–1537.
Esat, T.M., McCulloch, M.T., Chappell, J., Pillans, B., Omura, A., 1999. Rapid fluctuations in sea level recorded at Huon Peninsula during the penultimate deglaciation. Science 283 (5399), 197–201.
Fairbanks, R.G., 1989. A 17000 year glacio-eustatic sea-level record: influence of glacial melting rates on the Younger Dryas event and deep ocean circulation. Nature 342, 637–642.
Frank, M., O'Nions, R.K., Hein, J.R., Banakar, V.K., 1999. 60 Myr records of major elements and Pb–Nd isotopes from hydrogenous ferromanganese crusts: reconstruction of seawater paleochemistry. Geochimica et Cosmochimica Acta 63 (11–12), 1689–1708.
Galewsky, J., 1998. The dynamics of foreland basin carbonate platforms: tectonic and eustatic controls. Basin Research 10 (4), 409.
Galewsky, J., Silver, E., Gallup, C.D., Edwards, L., Potts, D., 1996. Foredeep tectonics and carbonate platform dynamics in the Huon Gulf, Papua New Guinea. Geology 24 (9), 819–822.
Gallup, C.D., Cheng, H., Speed, R., Taylor, F.W., Edwards, R.L., 2002. Direct determination of the timing of sea level change during termination II. Science 295 (5553), 310–313.
Grigg, R.W., Epp, D., 1989. Critical depth for the survival of coral islands: effects on the Hawaiian Archipelago. Science 243 (4891), 638–641.
Grootes, P.M., Stuiver, M., White, J.W.C., Johnsen, S., Jouzel, J., 1993. Comparison of oxygen isotope records from the GISP2 and GRIP Greenland ice cores. Nature 366, 552–554.
Hanebuth, T., Stattegger, K., Grootes, P.M., 2000. Rapid flooding of the Sunda Shelf: a late-glacial sea-level record. Science 288 (5468), 1033–1035.
Heinrich, H., 1988. Origin and consequences of cyclic ice rafting in the northeast Atlantic Ocean during the past 130,000 years. Quaternary Research 29, 143–152.
Hemming, S.R., Bond, G.C., Broecker, W.S., Sharp, W.D., Klas-Mendelson, M., 2000. Evidence from Ar40/Ar39 ages of individual hornblende grains for varying Laurentide sources of iceberg discharges 22,000 to 10,500 yr BP. Quaternary Research 54, 372–383.
Hohenegger, J., Yordanova, E., Hatta, Y., 2000. Remarks on West Pacific (Nummulitidae). Journal of Foraminifera Research 30, 3–28.
Imbrie, J., Hays, J.D., Martinson, D.G., McIntyre, A., Mix, A.C., Morley, J.J., Pisias, N.G., Prell, W.L., Shackleton, N.J., 1984. The orbital theory of Pleistocene climate: support from a revised chronology of the marine d18O record. In: Berger, A.L., Imbrie, J., Hays, J.D., Kukla, J., Saltzman, B. (Eds.), Milankovitch and Climate. Reidel, Dordrecht, pp. 269–305. Part 1.
Iryu, Y., Nakamori, T., Matsuda, S., Abe, O., 1995. Distribution of marine organisms and its geological significance in the modern reef complex of the Ryukyu Islands. Sedimentary Geology 99 (3–4), 243–258.
Jones, A.T., 1995. Geochronology of drowned Hawaiian coral reefs. Sedimentary Geology 99, 223–242.

Kienast, M., Hanebuth, T.J.J., Pelejero, C., Steinke, S., 2003. Synchroneity of meltwater pulse 1a and the Bolling warming: new evidence from the South China Sea. Geology 31 (1), 67–70.
Lambeck, K., Chappell, J., 2001. Sea level change through the last glacial cycle. Science 292 (5517), 679–686.
Lambeck, K., Esat, T., Potter, E., 2002. Links between climate and sea-levels for the past three million years. Nature 419, 199–206.
Lea, D.W., Martin, P.A., Pak, D.K., Spero, H.J., 2002. Reconstruction a 350 ky history of sea-level using planktonic Mg/Ca and oxygen isotope records from a Cocos Ridge core. Quaternary Science Reviews 283, 283–293.
Lea, D.W., Pak, D.K., Spero, H.J., 2003. Sea surface temperatures in the western equatorial Pacific during marine isotope stage 11. In: Droxler, A., Poore, R., Burckle, L. (Eds.), Earth's Climate and Orbital Eccentricity: The Marine Isotope Stage 11 Question. Geophysical Monograph Series. AGU, Washington, D.C., pp. 147–156.
Liu, P.J., Milliman, J.D., 2004. Reconsidering meltwater pulses 1A and 1B: global impacts of rapid sea level rise. Journal of Ocean University of China (Oceanic and Coastal Sea Research) 3 (2), 183–190.
Ludwig, K.R., Szabo, B.J., Moore, J.G., Simmons, K.R., 1991. Crustal subsidence rate off Hawaii determined from 234U/238U ages of drowned coral reefs. Geology 19 (2), 171–174.
Manheim, F.T., Lane-Bostwick, C.M., 1988. Cobalt in ferromanganese crusts as a monitor of hydrothermal discharge on the Pacific sea floor. Nature 335, 59–62.
MBARI Mapping Team, 2000. MBARI Hawaii Multibeam Survey, Digital Data Series No.2. Monterey Bay Aquarium Research Institute, Moss Landing.
Montaggioni, L.F., 1988. Holocene reef growth history in mid-plate high volocanic islands. Procceed. Sixth Intern. Coral Reef Symp, Australia, pp. 455–460.
Montaggioni, L.F., Cabioch, G., Gilbert, G.F., Bard, E., Faure, G., Dejardin, P., Recy, J., 1997. A 14,000 year continuous record of reef growth in a mid-Pacific island. Geology 25 (6), 555–559.
Moore, J.G., 1987. Subsidence of the Hawaiian ridge. In: Decker, R.D., Wright, T.L., Staufer, P.H. (Eds.), Volcanism in Hawaii. U.S. Geological Survey Professional Paper, Washington DC, pp. 85–100.
Moore, J.G., Fornari, D.J., 1984. Drowned reefs as indicators of the rate of subsidence of the island of Hawaii. Journal of Geology 92, 753–759.
Moore, J.G., Campbell, J.F., 1987. Age of tilted reefs, Hawaii. Journal of Geophysical Research 92, 2641–2646.
Moore, J.G., Clague, D.A., 1987. Coastal laval flows from Mauna Loa and Hualalai volcanoes. Bulletin of Volcanology 49 (6), 752–764.
Moore, J.G., Clague, D.A., 1992. Volcano growth and evolution of the island of Hawaii. Geological Society of American Bulletin 104, 1471–1484.
Moore, J.G., Chadwick, W.W.J., 1995. Offshore geology of Mauna Loa and adjacent areas, Hawaii. In: Rhodes, J.M., Lockwood, J.P. (Eds.), Mauna Loa Revealed: Structure, Composition, History, and Hazards. American Geophysical Union, Washington, D.C., pp. 21–44.
Moore, J.G., Ingram, B.L., Ludwig, K.R., Clague, D.A., 1996. Coral ages and island subsidence, Hilo drill hole. Journal of Geophysical Research 101 (NO. B5.), 11599–11605.
Pandolfi, J.M., 1996. Limited membership in Pleistocene reef coral assemblages from the Huon Peninsula, Papua New Guinea: constancy during global change. Paleobiology 22 (2), 152–176.
Pigram, C.J., Davies, H.L., 1987. Terranes and accretion history of the New Guinea orogen. BMR Journal of Australian Geology and Geophysics 10, 193–211.
Pirazzoli, P.A., Montaggioni, L.F., 1988. The 7,000 YR sea-level curve in French Polynesia: geodynamic implications for mid-plate volocanic islands. Proceedingsof the Sixth International Coral Reef Symposium, 3, pp. 467–472.
Riker-Coleman, K., Gallup, C., Webster, J.M., Cheng, H., Burr, G., Potts, D., Silver, E., Wallace, L.M., Edwards, L., 2004. Documentation of Carbonate Platform Drowning During MIS 4 in the Huon Gulf, Papua New Guinea. Eos Transactions Fall Meeting Supplement. American Geophysical Union, San Francisco. Abstract PP13A-0585.
Riker-Coleman, K., Gallup, C., Clague, D., Webster, J.M., Edwards, L., Cheng, H., 2005. New 230Th ages from the −400 m reef of northwestern Hawaii. Eos Transactions Fall Meeting Supplement. American Geophysical Union, San Francisco. Abstract PP21C-1574.
Sachs, J.P., Lehman, S.J., 1999. Subtropical North Atlantic temperatures 60,000 to 30,000 Years Ago. Science 286 (5440), 756–759.
Schlager, W., 1981. The paradox of drowned reefs and carbonate platforms. Geological Society of America Bulletin 92 (4), 197.
Sharp, W.D., Renne, P.R., 2006. The 40Ar/39Ar dating of core recovered by the Hawaii Scientific Drilling Project (phase 2), Hilo, Hawaii. Geochemistry, Geophysics,and Geosystems 6 (4). doi:10.1029/2004GC000846.
Szabo, B.J., Moore, G.J., 1986. Age of −360 m reef terrace, Hawaii, and the rate of late Pleistocene subsidence of the island. Geology 14 (11), 967–968.
Tager, D., Webster, J.M., Potts, D., Renema, W., Braga, J.C. and Pandolfi, J.M., in press. Community composition and dynamics of Pleistocene reefs during successive sea-level lowstands versus highstands Ecology Reports.
Thompson, W.G., Goldstein, S.L., 2005. Open-system coral ages reveal persistent suborbital sea-level cycles. Science 308 (5720), 401–404.
Wallace, L., 2002. Tectonic and Arc-Continent Collision in Papua New Guinea: Insights from Geodetic, Geophysical and Geologic Data. University of California, Santa Cruz. 278 pp.
Wallace, L.M., Stevens, C., Silver, E., McCaffrey, R., Loratung, W., Hasiata, S., Stanaway, R., Curley, R., Rosa, R., Taugaloidi, J., 2004. GPS and seismological constraints on active tectonics and arc-continent collision in Papua New Guinea: implications for mechanics of microplate rotations in a plate boundary zone. Journal of Geophysical Research 109 (B05404). doi:10.1029/2003JB002481.
Weaver, A.J., Saenko, O.A., Clark, P.U., Mitrovica, J.X., 2003. Meltwater Pulse 1A from Antarctica as a trigger of the Bolling–Allerod warm interval. Science 299 (5613), 1709–1713.
Webster, J.M., 2006. Coral reef evolution on rapidly subsiding margins: a unique record of drowning and backstepping. In: Pretcht, W.F., Mitch, H. (Eds.), Quaternary reefs and platforms: Bridging the gap between the ancient and the modern. Society for Sedimentary Geology (SEPM), Houston, Texas, p. 44. Short Course #19, Abstract.
Webster, J.M., Davies, P.J., 2003. Coral variation in two deep drill cores: significance for the Pleistocene development of the Great Barrier Reef. Sedimentary Geology 159, 61–80.
Webster, J.M., Clague, D.A., Coleman-Riker, K., Gallup, C., Burr, G., Braga, J.C., Potts, D., Moore, G.J., Winterer, E.L., Paull, C.K., 2003. Drowning of the −150 m reef off Hawaii: A casualty of global meltwater pulse 1A? Geological Society of America, GSA Seattle, US, p. 507 (Abstract).
Webster, J.M., Clague, D.A., Riker-Coleman, K., Gallup, C., Braga, J.C., Potts, D., Moore, J.G., Winterer, E.L., Paull, C.K., 2004a. Drowning of the −150 m reef off Hawaii: a casualty of global meltwater pulse 1A? Geology 32 (3), 249–252.
Webster, J.M., Wallace, L., Silver, E., Applegate, B., Potts, D., Braga, J.C., Coleman-Riker, K., Gallup, C., 2004b. Drowned carbonate platforms in the Huon Gulf, Papua New Guinea. Geochemistry, Geophysics and Geosystems 5 (11), Q11008. doi:10.1029/2004GC000726.
Webster, J.M., Wallace, L., Silver, E., Potts, D., Braga, J.C., Renema, W., Riker-Coleman, K., Gallup, C., 2004c. Coralgal composition of drowned carbonate platforms in the Huon Gulf, Papua New Guinea; implications for lowstand reef development and drowning. Marine Geology 204 (1–2), 59–89.
Webster, J.M., Wallace, L., Clague, D., Braga, J.C., 2007. Numerical modeling of the growth and drowning of Hawaiian coral reefs during the last two glacial cycles (0–250 ka). Geochemistry, Geophysics and Geosystems 8 (Q03011). doi:10.1029/2006GC001415.
Wilson, J., 1963. A possible origin of the Hawaiian Islands. Canadian Journal of Physics 41, 863–870.
Yokoyama, Y., Esat, T.M., Lambeck, K., 2001. Coupled climate and sea-level changes deduced from Huon Peninsula coral terraces of the last ice age. Earth and Planetary Science Letters 193 (3–4), 579–587.